Received: 5 June 2020 | Revised: 10 January 2021 | Accepted: 21 January 2021

DOI: 10.1002/aqc.3582

SPECIAL ISSUE ARTICLE

WILEY

Classifying flow regimes of the Amazon basin

Sharmin F. Siddiqui[1] | Xavier Zapata-Rios[2,3] | Sandra Torres-Paguay[2,3] | Andrea C. Encalada[4] | Elizabeth P. Anderson[5] | Mark Allaire[1] | Carolina Rodrigues da Costa Doria[6] | David A. Kaplan[1]

[1]Department of Environmental Engineering Sciences, University of Florida, Gainesville, FL

[2]Departamento de Ingeniería Civil y Ambiental, Facultad de Ingeniería Civil y Ambiental, Escuela Politécnica Nacional, Quito, Ecuador

[3]Centro de Investigaciones y Estudios en Recursos Hídricos (CIERHI), Escuela Politécnica Nacional, Quito, Ecuador

[4]Instituto BIOSFERA, Laboratorio de Ecología Acuática, Universidad San Francisco de Quito (USFQ), Quito, Ecuador

[5]Department of Earth and Environment and Institute of Environment, Florida International University, Miami, FL

[6]Laboratory of Ichthyology and Fisheries - Department of Biology, Universidade Federal de Rondonia, Porto Velho, Rondônia, Brazil

Correspondence
David Kaplan, Department of Environmental Engineering Sciences, University of Florida, 1953 Museum Road, Gainesville, FL, 32601, USA.
Email: dkaplan@ufl.edu

Funding information
Escuela Politécnica Nacional, Grant/Award Number: PIMI-17-04; John D. and Catherine T. MacArthur Foundation, Grant/Award Number: 16-1607-151; National Science Foundation, Grant/Award Number: DGE-1842473

Abstract

1. The Amazon River basin contains a vast diversity of lotic habitats and accompanying hydrological regimes. Further understanding the spatial distribution of flow regimes across the Amazon can be useful for recognizing riverine ecohydrological processes and informing river management and conservation, especially in areas with limited or inconsistent streamflow monitoring.
2. This study compares four inductive approaches for classifying streamflow regimes across the Amazon using an unprecedented compilation of streamflow records from Bolivia, Brazil, Colombia, Ecuador, and Peru.
3. Inductive classification schemes use attributes of streamflow data to categorize river reaches into similar classes, which then may be generalized to understand streamflow behaviour at the basin scale. In this study, classification was accomplished through hierarchical clustering of 67 flow metrics calculated using indicators of hydrologic alteration (IHA) and daily streamflow data from median annual hydrographs (MAHs) for 404 stations (representing >7,000 station-years) across five Amazonian countries.
4. Classification was performed using both flow magnitude-inclusive and flow magnitude-independent datasets. For flow magnitude-independent methods, optimal solutions included six or seven primary hydrological classes for IHA and MAH datasets; for approaches that retained magnitude, variance was sufficiently large to prevent convergence to a specific number of classes.
5. Across methods, class membership was strongly associated with the timing, frequency, and rate of change of flow, and spatially coherent clusters were associated with seasonal, elevational, and stream-order gradients. These results highlight the diversity of flow regimes across the Amazon and provide a framework for studying relationships between hydrological regimes and ecological responses in the context of changing climate, land use, and human-induced hydrological alteration.
6. The methodology applied provides a data-driven approach for classifying flow regimes based on observed data. When coupled with ecological knowledge and expertise, these classifications can be used to develop ecohydrologically informed and management-relevant conservation practices.

KEYWORDS
catchment management, classification, ecohydrology, flow metrics, hydrographs, river, streamflow, tropical, watershed

1 | INTRODUCTION

Tropical basins such as the Amazon, Mekong, and Congo are recognized for their immense size, biodiversity, social–cultural diversity, and range of distinct ecosystems (Abell et al., 2008; Coomes, Takasaki, Abizaid, & Barham, 2010). These large river basins facilitate countless ecosystem services at the local, regional, and global scales, including food supply, navigation, flood regulation, and carbon sequestration (Aylward et al., 2005), and they support nearly one-third of the world's freshwater fish species (Winemiller et al., 2016). Tropical river networks traverse a range of environments (Gupta, 2008), intersecting diverse landscapes and thus facilitating the success and movement of riparian organisms (Winemiller et al., 2016). Hydrological processes control floodplain dynamics (Bonnet et al., 2008; de Paiva et al., 2013; Fleischmann, de Paiva, Collischonn, Sorribas, & Pontes, 2016), fishery yields (Castello, Isaac, & Thapa, 2015; Isaac, Castello, Santos, & Ruffino, 2016), biogeochemical cycling (Junk et al., 2011), and material transport (Dunne, Mertes, Meade, Richey, & Forsberg, 1998; Fassoni-Andrade & de Paiva, 2019; Filizola & Guyot, 2009). The maintenance of the hydrological regime thus maintains ecological functioning and ultimately interfaces with social, cultural, and economic activities (Coomes, Lapointe, Templeton, & List, 2016; Coomes et al., 2010). Critically, accelerated human activities in the Amazon, such as hydropower development, land cover change, mining, and climate change are altering the hydrology of Earth's largest basins and increasingly threaten the stability of freshwater ecosystems (Castello & Macedo, 2016). In this context, relating quantifiable aspects of the flow regime to environmental flow criteria can help maintain ecosystem processes in freshwater ecosystems, amidst historic and continuing human alteration (Lima et al., 2014; Poff et al., 2010; Yarnell et al., 2020).

As the largest catchment in the world, the Amazon basin produces one-fifth of global river discharge (Salati & Vose, 1984) and is globally important in the regulation of large-scale atmospheric, hydrological, and biotic interactions (Werth, 2002). Large elevation gradients across the Amazon shape the behaviour and distribution of hydrological flow regimes through physioclimatic and geomorphological features (Encalada et al., 2019; Freeman, Pringle, & Jackson, 2007; McClain & Naiman, 2008), producing a range of diverse landscapes, including montane and submontane forests (McClain & Naiman, 2008), savannas (Malhado, Pires, & Costa, 2010), and wetland ecosystems (Hess et al., 2015). The Amazon basin is characterized by marked seasonality and spatial variation in rainfall (Espinoza Villar et al., 2009; Liebmann & Marengo, 2001; Marengo, 2004), strongly driving river pulsing, floodplain hydrology, and ecology (Hamilton, Sippel, & Melack, 2002; Mertes et al., 1995) and maintaining habitat for aquatic and terrestrial species (Castello & Macedo, 2016). Hydrological connectivity regulates the structure and functioning of Amazonian freshwater ecosystems and facilitates the survival, speciation, and migration of freshwater species through lateral and longitudinal connectivity (Anderson et al., 2018; Castello & Macedo, 2016).

Comprehensive biodiversity data enable the development of effective conservation measures and targets (Landeiro, Bini, Melo, Pes, & Magnusson, 2012), yet species-rich biodiversity hotspots such as the Amazon often lack high-quality biological information (Hopkins, 2007). The challenge of collecting large quantities of biodiversity data in mega-diverse basins is limited by time, labour, and resources, and is potentially outpaced by high rates of speciation (Dias, Cornu, Oberdorff, Lasso, & Tedesco, 2013) and human degradation (Castello & Macedo, 2016). For river ecosystems, a more effective and resource-efficient approach may be leveraging the availability of hydrological data to relate flow regime characteristics to the requirements and life-cycle histories of aquatic and riparian species (Bunn & Arthington, 2002). At the basin scale, identifying shared and unique characteristics among Amazon rivers can provide insights into the hydrological requirements of species confined to a specific range or biological niche, as well as the movement of aquatic species that rely on longitudinal or lateral connectivity (Junk, Bayley, & Sparks, 1989). For instance, the seasonal flood pulse is synchronized with the life cycles of many fish, macroinvertebrates, and amphibians (Junk, 2013), and many riparian species are accustomed to spatial and temporal patterns of natural flow variability.

Spanning eight countries and one territory, the Amazon basin currently lacks sufficient intergovernmental agreements for coordinated streamflow monitoring and inter-basin management (Junk, 2013), making it difficult to manage water resources across boundaries. In addition, the availability of long-term daily streamflow observations is still relatively sparse in tropical basins, including the Amazon (Do, Gudmundsson, Leonard, & Westra, 2018; Wohl et al., 2012). There is a strong need for widespread and consistent streamflow monitoring in the Amazon, and this need is partly motivated by the potential ecological insights that may be gained by doing so. Understanding the spatial distribution of streamflow patterns across the Amazon can provide insight into river functioning at the ecosystem scale and inform aquatic conservation efforts that prioritize the natural flow regime (Poff et al., 1997) and the maintenance of free-flowing rivers (Anderson, Osborne, et al., 2019).

For a region such as the Amazon basin, with a diversity of flow regimes, hydrological classification can be a useful tool for better understanding similarities and differences in riverine ecohydrological processes (Knoben, Woods, & Freer, 2018). Hydrological classification is the systematic arrangement of rivers into groups with similar flow regime characteristics and can be used to characterize flow variability, streamline water resources management, explore flow–ecology

relationships, prioritize conservation efforts, and transfer knowledge to data-scarce regions (Olden, Kennard, & Pusey, 2012). For example, the classification of river types is a primary step in the ecological limits of hydrologic alteration (ELOHA) framework, developed by The Nature Conservancy to determine and implement environmental flows at the regional scale (Poff et al. 2010). The ELOHA framework provides a foundation for developing and testing hypotheses about flow and ecological relationships, but it first requires the collection of long-term, spatially comprehensive streamflow data and the classification of ecohydrologically similar river types.

Hydrological classification approaches are generally divided into inductive and deductive methods, both of which aim to capture shared patterns among streamflow time series and provide insight into characteristics of the flow regime (Olden et al., 2012). Deductive methods assign landscape units to classes and assume that the shared physical attributes of a basin – such as topography, climate, and geomorphology – extend to similar flow patterns. For example, climate at the global scale regulates humidity, seasonality, and temperature, which interact to produce flow regimes that reflect local water and energy budgets (Knoben et al., 2018). Taken together, catchment climate, topography (Encalada et al., 2019), and geomorphological features (Lilly, 2010) combine to create distinct river hydropatterns that directly drive ecosystem structure, composition, and function, and influence human societies from local to global scales (Anderson, Jackson, et al., 2019). In contrast, inductive classification methods are applied directly to a set of defined streamflow metrics, which should be identifiable, robust, consistent across catchments, representative of catchment behaviour, and yield discriminatory power in differentiating between classes (McMillan, Westerberg, & Branger, 2017). Inductive classification techniques require long-term streamflow data that is both spatially and temporally representative of the system and assign hydrological units to classes that maximize within-group similarity and minimize similarity between groups. The resulting classification organizes rivers into similar groups that are presumed to share similar ecological response relationships, enabling the determination of previously unknown flow–ecology relationships, and the identification of key environmental flow criteria to maintain ecological function (Poff et al., 2010).

Previous classification schemes in the Amazon basin have focused on water chemistry, hydraulics, wetlands, and rainfall regimes, and provide useful frameworks for understanding the geological and topographical drivers that yield diverse flow patterns (Table 1). For example, Junk et al. (2011) extended the wetland classification system proposed by Brinson (1993) to devise an Amazon-specific taxonomic wetland classification system based on climatic, hydrological, biogeochemical, and botanical factors, resulting in 14 major wetland types. Filizola and Guyot (2009) provided four station hydrographs representative of hydrological regimes in the Amazon River basin, highlighting differences in the magnitude and onset of the wet season. Venticinque et al. (2016) connected hierarchical stream classification to the distribution of fish spawning areas. Beyond these studies, no holistic efforts have been made to classify Amazonian flow regimes; these vary across the basin, where large gradients in flow magnitude, variability, and timing are so strongly tied to ecosystem structure and function.

In this context, the objective of this study was to characterize patterns of variation in natural flow regimes in order to capture unique and shared streamflow characteristics relevant to river ecology. This study leverages an unprecedented compilation of streamflow records from Bolivia, Brazil, Colombia, Ecuador, and Peru to develop the first inductive classification of streamflow across the Amazon basin (French Guiana, Guyana, Suriname, and Venezuela were not included), and highlights flow metrics that are meaningful at the basin scale. The resulting work describes a set of four flow classifications assembled through distinct streamflow indicator datasets, each of which highlights salient features of Amazonian flow regimes.

2 | METHODS

Our inductive classification framework is summarized in Figure 1. Station flow records were used to create two classification datasets for each station: one using 67 indicators of hydrologic alteration (IHA) and environmental flow component (EFC) metrics, derived from long-term flow records (Richter, Baumgartner, Powell, & Braun, 1996), and the other using median annualized hydrographs (MAHs). Although magnitude is a critical and structuring component of the flow regime, we hypothesized that the large variance in discharge across the Amazon basin (approximately five orders of magnitude) could potentially mask other flow regime characteristics when assessed at the basin scale. Thus, two additional datasets were created to minimize the influence of flow magnitude: one using a subset of 29 flow magnitude-independent (MI) IHA/EFC parameters and the other using normalized MAHs (see further details in Section 2.2). Hierarchical clustering was applied to each of the four datasets, and the resulting output classes were compared within and across methods. All analyses were performed in ARCGIS 10.6 and R STUDIO 3.5.1.

2.1 | Streamflow data collection and preparation

Daily streamflow data were acquired for Bolivia, Brazil, Colombia, Ecuador, and Peru through the following databases: SO HYBAM (http://www.ore-hybam.org), Agência Nacional de Águas (http://www.ana.gov.br), IDEAM (http://www.ideam.gov.co), and INAMHI (http://www.serviciometeorologico.gob.ec). The initial dataset included 537 streamflow stations, and stations were included or excluded based on their ability to meet data quality criteria (Table 2). Streamflow records of fewer than three complete years were removed. Data from the remaining stations were processed and quality controlled as described below, yielding a total of 404 stations (representing 7,825 station-years) over a 90-year period (1928–2018) (Figure 2). The average station record was 19.2 ± 12.6 (SD) years. Data were next assessed for completeness on a year-by-year basis. Years for which the data were less than 80% complete (i.e. <292 days

TABLE 1 Existing classification schemes within the Amazon basin

Classification method	Type of classification	No. of classes	Reference
Principal components analysis	Water chemistry	3	Ríos-Villamizar, Piedade, Da Costa, Adeney, & Junk, 2013; Sioli, 1957
St. Venant	Flood wave	5	Getirana & Paiva, 2013
K-means hierarchical clustering	Cloud	5	Giangrande, Wang, & Mechem, 2020
Ward's hierarchical clustering	Streamflow and precipitation	4	Laraque, Ronchail, Cochonneau, Pombosa, & Guyot, 2007
Taxonomic	Wetlands	14	Junk et al., 2011
Inspection of sediment yield	Streamflow	4	Filizola & Guyot, 2009

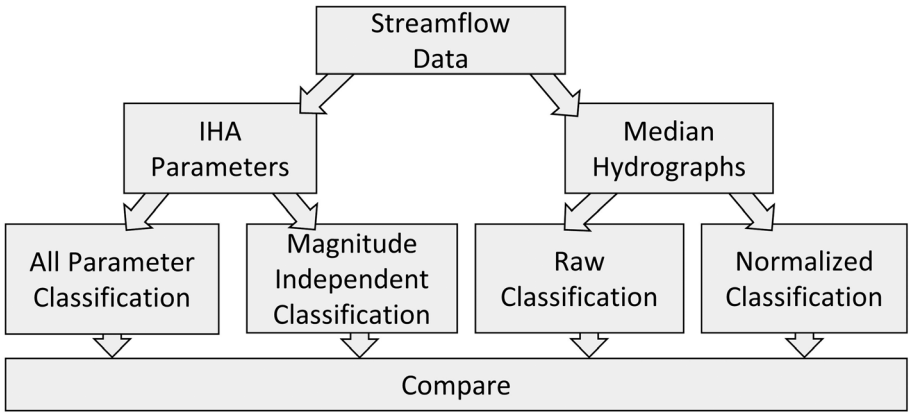

FIGURE 1 Inductive classification framework. Streamflow data were characterized by two datasets: (i) indicators of hydrologic alteration (IHA)/environmental flow component (EFC) parameters; and (ii) median annualized hydrographs. Both datasets were used to create input datasets with and without the influence of discharge magnitude. Resulting classes were then compared to reveal salient attributes of the flow regime captured by each approach

TABLE 2 Summary of streamflow station number during data processing (see data sources in main text)

	Bolivia	Brazil	Colombia	Ecuador	Peru	Total
Acquisition	38	366	54	20	59	537
Removal of stations with <3 years data AND/OR ≤80% data/year	−5	−76	−8	−2	−6	−97
Removal of stations following interpolation and homogenization	−10	−2	0	0	−1	−13
Removal of potentially dam-altered stations	0	−12	0	−3	−8	−23
Total	23	276	46	15	44	404

Note: The 'Acquisition' row refers to the number of initial daily streamflow stations. Prior to this step, duplicate stations between countries were compared and consolidated, and stations with no streamflow data were removed. The following rows reflect stations that were removed at each step. The 'Total' row and column reflect the final number of stations for that country and processing step, respectively.

of data in a calendar year) were removed. For years with at least 80% data completeness, gaps were filled using multiple linear regression (Beauchamp, Downing, & Railsback, 1989). Predictor variables were selected as nearby stations that contained data during the missing data gap through a forward model selection algorithm. If the regression model yielded an adjusted R^2 value of ≥0.7 for predicted flow, then the interpolated gap values were accepted. If multiple linear regression yielded adjusted R^2 values of <0.7 and the gap was shorter than 10 days, it was filled using linear interpolation. If the gap was greater than 10 days and could not be predicted through multiple linear regression, the year was removed from the analysis.

Streamflow data were further filtered to obtain natural flow records by removing stations potentially affected by dams. As a conservative estimate, any stations within 200 km (Cartesian distance) of an operational dam were first identified as potentially affected (Valle & Kaplan 2019). From this list, station removal was assessed using available dam construction and operation years and pre- and post-dam flow record at each potentially affected station (Anderson et al., 2018; ANEEL, 2019; RAISG, 2012; Timpe & Kaplan, 2017). In cases where dam construction dates were unavailable or the dam pre-dated the available period of flow data, dam impacts were assessed by comparing contemporaneous flow

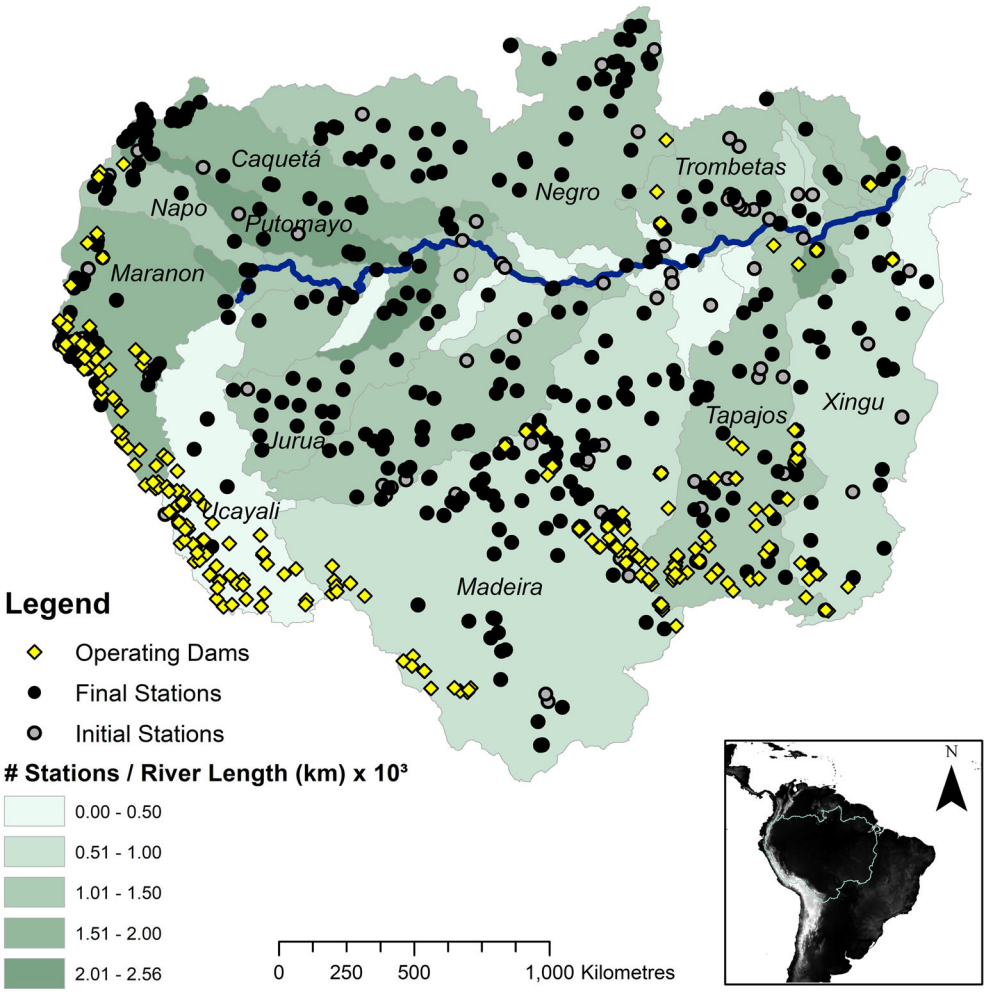

FIGURE 2 Spatial distribution of streamflow stations and operational dams across the topographical Amazon River basin (excludes the Araguaia–Tocantins basin). Black circles represent stations included in the analysis, grey circles represent stations that did not meet data-quality criteria, and yellow diamonds represent operational dams (ANEEL, 2019; RAISG, 2012). Major sub-catchments are shaded based on stream gauging density (stations per tributary length, based on 3rd- to 10th-order streams). Mainstem, tributary, and digital elevation model (DEM) layers were obtained from Oak Ridge National Laboratory (Mayorga, Logsdon, Ballester, & Richey, 2012)

records of upstream and downstream stations in both the pre- and post-dam periods, when available (Solans & Poff, 2013). If dam influence was confirmed or strongly suspected, only pre-dam streamflow data (if available) were retained in the analysis (Table S1).

2.2 | Flow indices and mean annual hydrographs

A variety of ecohydrological flow indices were calculated and median annual hydrographs were developed for each of the 404 stations described above. INDICATORS OF HYDROLOGIC ALTERATION (IHA; Nature Conservancy, 2009) provides a standardized approach to calculating the hydrological indicators and EFCs that represent characteristics of flow time-series data (Richter et al., 1996). Combined, the IHA and EFC metrics characterize the flow regime using 67 indicators across 10 broad flow categories, with each indicator directly related to known ecohydrological relationships (Nature Conservancy, 2009). Given the choice of hundreds of available flow metrics, IHA and EFC metrics were selected because of their relevance to ecological functioning across multiple timescales and encompassing primary components of the flow regime, their ability to be altered by anthropogenic basin modification (Arias et al., 2020; Lima et al., 2014; Timpe & Kaplan, 2017), and their subsequent ability to manage and restore environmentally sound flow regimes (Poff et al., 2010). The 67 IHA and EFC parameters were calculated for each complete year of data across all stations. For each parameter, mean and standard deviation metrics were tabulated on a calendar-year basis to retain seasonal differences between stations. IHA and EFC parameters are summarized in Tables 3 and 4, with the 29 flow magnitude-independent parameters (described below) noted in *italics*. Low and high pulses are defined as the number of days fewer than or greater than a specified threshold (one standard deviation from mean annual flow). Rates refer to the average positive or negative differences between consecutive daily values. Further details of IHA and EFC calculations are detailed in the IHA 7.1 user's manual (Nature Conservancy, 2009). Following the approach of Hannah, Smith, Gurnell, and McGregor (2000), median annualized hydrographs were calculated for each flow station using the median flow for each day over all available calendar years. Both raw and normalized (i.e. transformed between 0 and 1) hydrographs were used for inductive classification. Normalized hydrographs were also used to aid in the visualization of results across all four clustering approaches using the GGMAP package in R (Kahle & Wickham, 2019).

TABLE 3 Indicators of hydrologic alteration (IHA) parameters

Magnitude of monthly flow conditions	Magnitude/duration of annual extreme flow conditions	Timing of annual extreme flows	Frequency/duration of high/low pulses	Rate/frequency of hydrological changes
January	1-day min.	*Date of max.*	*Low pulse count*	*Rise rate*
February	3-day min.	*Date of min.*	*Low pulse duration*	*Fall rate*
March	7-day min.		*High pulse count*	*No. of reversals*
April	30-day min.		*High pulse duration*	
May	90-day min.			
June	1-day max.			
July	3-day max.			
August	7-day max.			
September	30-day max.			
October	90-day max.			
November	*No. of 0-flow days*			
December	*Baseflow index*			

Note: Italicized parameters were included in the flow magnitude-independent classification. Further details are available from Nature Conservancy (2009).

TABLE 4 Environmental flow component (EFC) parameters

Magnitude of monthly low flows	Extreme low flows	High flow pulses	Small floods	Large floods
January	*Frequency of extreme low flows*	*Frequency of extreme high flows*	*Frequency of small floods*	*Frequency of larger floods*
February	*Duration of low flows*	*Duration of high flows*	*Duration of small floods*	*Duration of large floods*
March	Peak flow	Peak flow	Peak flow	Peak flow
April	*Date of min. flow*	*Date of peak flow*	*Date of peak flow*	*Date of peak flow*
May		*Rise Rate*	*Rise Rate*	*Rise Rate*
June		*Fall Rate*	*Fall Rate*	*Fall Rate*
July				
August				
September				
October				
November				
December				

Note: Italicized parameters were included in the flow magnitude-independent classification. Further details are available from Nature Conservancy (2009).

2.3 | Streamflow classification

Inductive classification was performed using both annualized hydrographs and derived IHA and EFC parameters (Figure 1). First, flow classification was performed using all 67 IHA/EFC parameters (hereafter referred to as IHA:All) and then repeated using only parameters that were independent of magnitude (IHA:MI; Tables 3 and 4). Next, classification was performed on raw MAHs (MAH:Raw) and repeated using normalized hydrographs (MAH:Normalized). Clustering using both flow magnitude-inclusive and flow magnitude-independent approaches was intended to account explicitly for the influence of magnitude in driving flow regime while also elucidating other characteristics of the flow regime.

For each dataset, streamflow stations were grouped into classes using hierarchical clustering (Haaf & Barthel, 2018), which clusters the most similar station groups until all groups are connected in a nested structure, often presented as a dendrogram (Olden et al., 2012). The method of Ward (1963) was applied to establish groups based on a minimum variance criterion and the gap statistic was used to select the optimal number of classes (Auerbach et al., 2016; Tibshirani, Walther, & Hastie, 2001). The gap statistic was applied to select a parsimonious number of classes that minimized variance within each class. The gap statistic value is represented as the difference between intragroup variation at class k if there was no significant difference in variation across group members (null distribution) and the actual intragroup variation when linked (Tibshirani et al., 2001). When all

standard deviations are larger than the computed gap statistics, k is set to 1. Conceptually, this value determines the inflection point where an increase in the number of classes does not lead to a significant decrease in variation (Tibshirani et al., 2001).

To assess within-group hydrological similarity, the correlation among annualized hydrographs within each cluster was quantified across the four sets of results. To do so, the normalized cross correlation (NCC) was calculated for each set of clusters (Iglesias & Kastner, 2013), taken as the station-weighted average among all pairwise correlations in a given class. To assess the strength of a set of classes, the Jaccard Index (JI) was used, which varies from 0 to 1, with higher values indicating a greater likelihood that a station belongs to its assigned class, based on repeated sampling. The JI was used as a measure of homogeneity across multiple bootstrap iterations (B = 100) of each resulting classification (Auerbach et al., 2016; Hennig, 2014). Although MAH-based classifications did not use derived IHA/EFC parameters, selected parameters were summarized across all classes in each of the four methods for comparison.

Following the approach of Olden and Poff (2003), a principal components analysis (PCA) was applied as a supplementary analysis to identify IHA parameters that described primary sources of variation among streamflow classes. Within each PCA, it was assumed that for any randomly distributed dataset, the expected contribution of all variables would be equal. The actual contribution for an input dataset is defined as the squared eigenvalue coordinate of the variable (with respect to its PC axis) divided by the squared distances for all variables. The actual contribution was calculated for each variable (using the FACTOEXTRA package in R; Kassambara & Mundt, 2019), providing a ranking of the strongest drivers of classification.

2.4 | Comparison with the Global Rivers Classification product

The derived classifications were compared with the Global River Classification (GloRiC) product from HydroSHEDS (Ouellet-Dallaire, Lehner, Sayre, & Theime, 2019). This global dataset provides classification at the river-reach scale (www.hydrosheds.org/page/gloric). Classification results were compared specifically with the GloRiC hydrological classification, which is considered an inductive classification based on long-term average discharge and flow regime variability modelled using WATERGAP (Döll, Kaspar, & Lehner, 2003). The GloRiC framework includes 15 distinct hydrological classes with five levels of magnitude (Q), very low (0.1–10 $m^3\ s^{-1}$), low (10–100 $m^3\ s^{-1}$), medium (100–1,000 $m^3\ s^{-1}$), high (>1,000–10,000 $m^3\ s^{-1}$), and very high (>10,000 $m^3\ s^{-1}$), and three levels of flow variability index (V), low ($V < 2$), medium ($2 < V < 3$), and high ($V > 3$). Variability is defined as the maximum of the long-term average monthly discharge divided by the long-term average discharge. To standardize and compare the results from this analysis with GloRiC, an Amazon-specific GloRiC classification was created where each flow station was assigned to a respective GloRiC class. In cases of clear misalignment between GloRiC river classification and station assignment, stations were inspected and GloRiC classes reassigned to more likely adjacent river reaches. Finally, NCC values were calculated for stations assigned to each class in the Amazon-GloRiC classification and qualitatively compared with the classification sets generated in this analysis, with respect to spatial distribution and NCC.

3 | RESULTS

Hierarchical clustering of the four datasets yielded differences in the optimal number of classes, station distributions within classes, and subsequent differences in the spatial patterns of class membership. For approaches that retained magnitude (IHA:All and MAH:Raw), substantial variation in discharge across the basin prevented convergence to a statistically optimal number of classes (i.e. all rivers were grouped into a single class). In contrast, the two flow magnitude-independent datasets both converged, with six and seven classes recommended for the IHA:MI and MAH:Normalized datasets, respectively (Figure 3). Notably, these flow magnitude-independent approaches retained a magnitude 'signature', yielding flow classes at least partly organized by discharge (Figures 4–7; Table 5) owing to inherent collinearity among many flow regime characteristics (Olden & Poff, 2003). To facilitate comparison among the four approaches in the following sections, six classes were arbitrarily selected for illustrating the results from the two magnitude-inclusive datasets. Dendrograms for all datasets are shown in Figures S1–S4.

Table 5 presents summary statistics for all methods and resulting classes, including IHA parameters that strongly contributed to variation in the PCA (Figures S5 and S6). The distribution of flow stations across classes varied widely by method, with the most equal distributions for the flow magnitude-independent approaches and the most unequal distribution for MAH:Raw, which had three classes each with only three stations. Normalized cross-correlations (NCCs) were also highest for flow magnitude-independent approaches (with station-weighted means of 0.65 and 0.83 for IHA:MI and MAH:Normalized, respectively), compared with flow magnitude-inclusive approaches (with station-weighted means of 0.49 and 0.36 for IHA:All and MAH:Raw, respectively). Table 5 also shows a consistent trend of decreasing mean elevation and number of reversals, and increasing stream order, 90-day maximum, and rise rates, with increasing class number. This pattern suggests a strong physiographical driver of class membership, with class 1 generally representing higher-elevation, lower-magnitude streams and class 6 representing large, lowland rivers. Of note, a trend from low- to high-magnitude mean class discharge (characterized here as 90-day maximum) was maintained for both flow magnitude-inclusive and flow magnitude-independent datasets. There was a large variation in the timing of flow minima and maxima (e.g. maximum flow dates ranging from day 62 to day 180 and minimum flow dates ranging from day 37 to day 317 across classes and approaches), despite the relatively low contribution of explicit timing-based variables in PCA loadings (Figures S5 and S6).

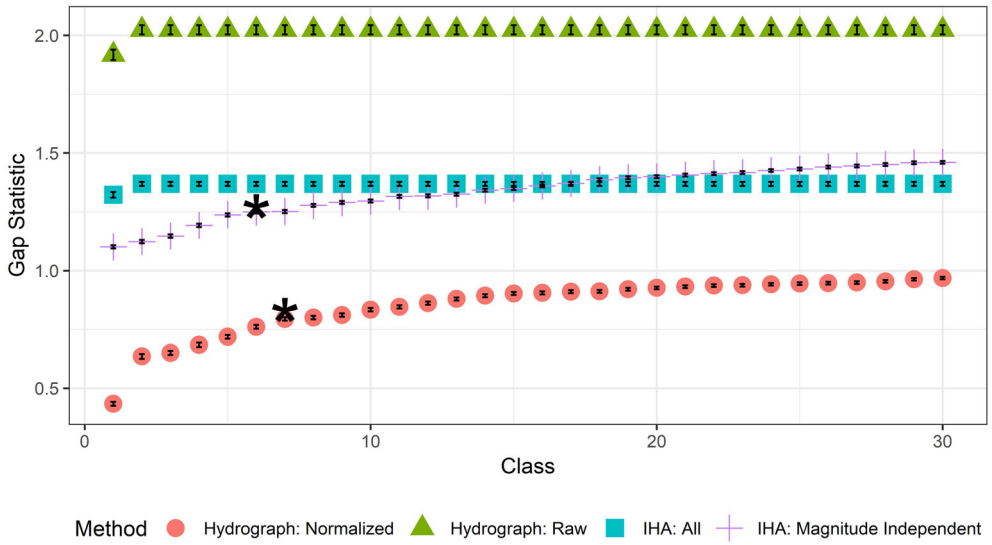

FIGURE 3 Gap statistic determination for all classification approaches. MAH:Normalized and IHA:MI were partitioned into six and seven classes, respectively (denoted by *); IHA:All and MAH: Raw did not converge to an optimal class number

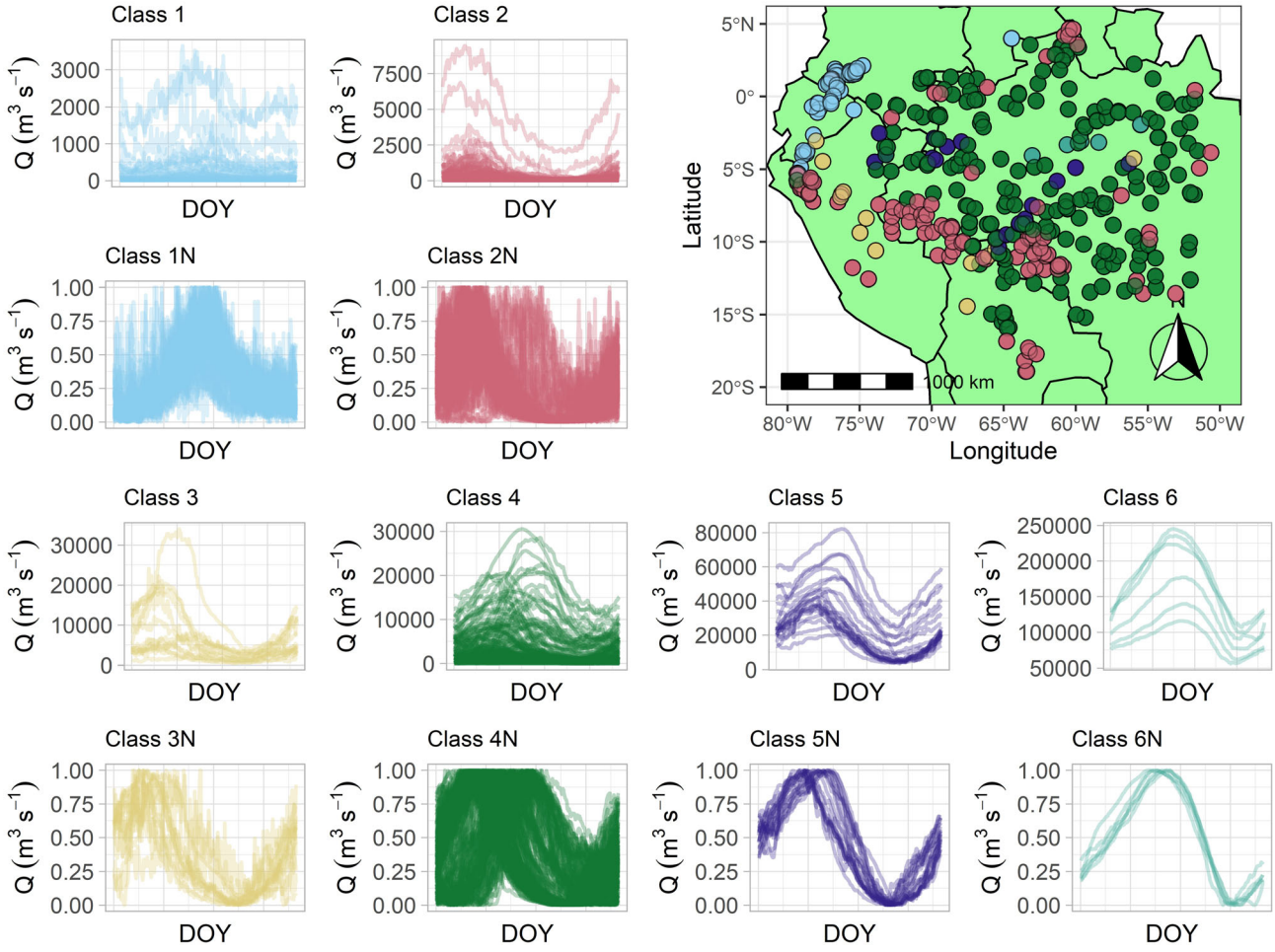

FIGURE 4 Classification results for magnitude-inclusive indicators of hydrologic alteration parameters (IHA:All). Normalized hydrographs are included for each class, denoted by 'N'. DOY refers to calendar day of the year. Classes are numbered from lowest to highest maximum within-class discharge. Geographically coherent flow regime clusters include class-1 stations (light blue) in the highest-elevation regions of the Colombian and Ecuadorian Amazon (>1,000 m a.s.l.), class-3 stations (yellow) in the Peruvian and Bolivian Amazon, and class-5 and -6 stations (dark blue and turquoise) along the Amazon and major tributary mainstems (e.g. the Madeira, Tapajos, and Solimoes)

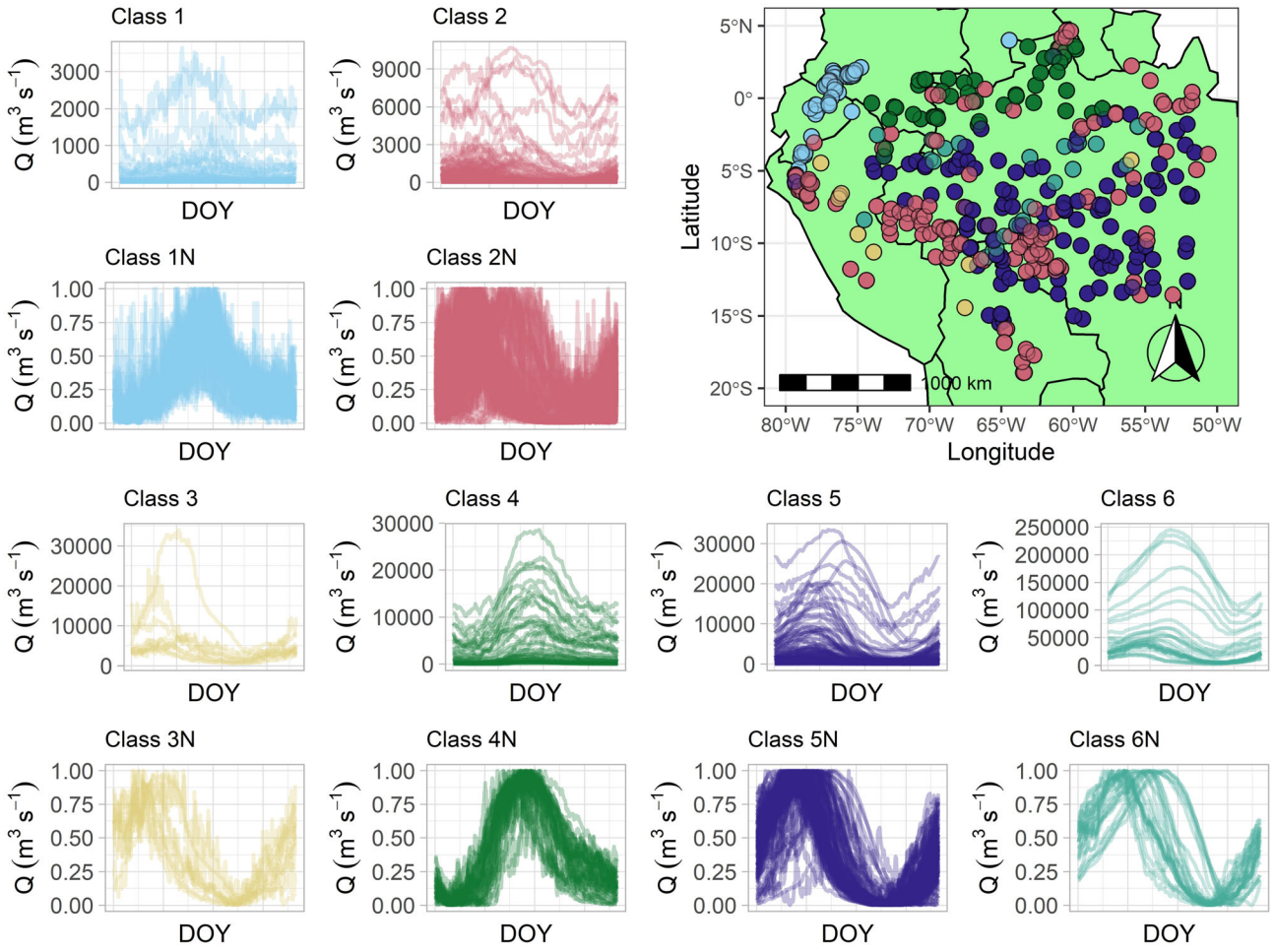

FIGURE 5 Classification results for flow magnitude-independent indicators of hydrologic alteration parameters (IHA:MI). Normalized hydrographs for each class are denoted by 'N'. DOY refers to calendar day of the year. Classes are numbered from lowest to highest maximum within-class discharge. Geographically coherent flow regime clusters include class-1 stations (light blue) in the highest-elevation regions of the Colombian and Ecuadorian Amazon (>1,000 m a.s.l.), class-4 stations (green) across the northern Amazon (500–1,000 m), and class-6 stations (purple) along the Amazon and major tributary mainstems (e.g. the Madeira, Tapajos, and Solimoes)

Figures 4 and 5 present median annualized hydrographs and spatial distribution of flow classes for the two IHA-based approaches; MAH-based results are summarized in Figures 6 and 7. For each pair of hydrographs, the upper panel shows raw MAHs and the bottom panel provides normalized MAHs to aid in visualization. It is important to reiterate that Figures 4–7 represent unique hierarchical classifications using specific input datasets (i.e. 67 or 29 IHA parameters in Figures 4 and 5 and 365 median daily flow values from raw and normalized MAHs in Figures 6 and 7). Taken together, these figures illustrate differences in hydrograph magnitude, seasonality, and flashiness (i.e. short-term flow variance, rate of change, and number of reversals) across classes and between methods. In general, flashiness was highest in lower-magnitude, class-1 and -2 streams and decreased with class number (associated with increasing stream order, decreasing elevation, etc.). Classes were also aligned with trends in flow timing, with flow maxima that ranged from February (e.g. class 3 in Figures 4 and 5) to July (e.g. class 2 in Figure 5). To further illustrate this seasonal timing gradient, the mean dates of flow maxima are presented in Figure 8, showing a bimodal distribution of flow maxima in February/March (south of the mainstem Amazon), June/July (north of the mainstem), and very rarely between August and December in higher-elevation upland rivers with relatively low seasonal variation. Differences in the number of stations per class (e.g. many versus few stations in IHA:MI class 2 versus class 3, respectively; Figure 5) and relative within-class MAH similarity (e.g. low versus high in those same classes) were also evident and align with the statistics listed in Table 5.

Notably, classes developed using the two flow magnitude-independent approaches (Figures 5 and 7) included streams with a very wide range of flows. For instance, the 48 stations in class 7 of the MAH:Normalized approach had very strongly correlated MAHs (NCC = 0.86) despite spanning four orders of magnitude (Figure 7). In other words, flow magnitude-independent approaches were successful at grouping together stations with similar hydrograph shapes but did not strongly differentiate 'small' and 'large' rivers. Not surprisingly, flow classes for the flow magnitude-inclusive approaches

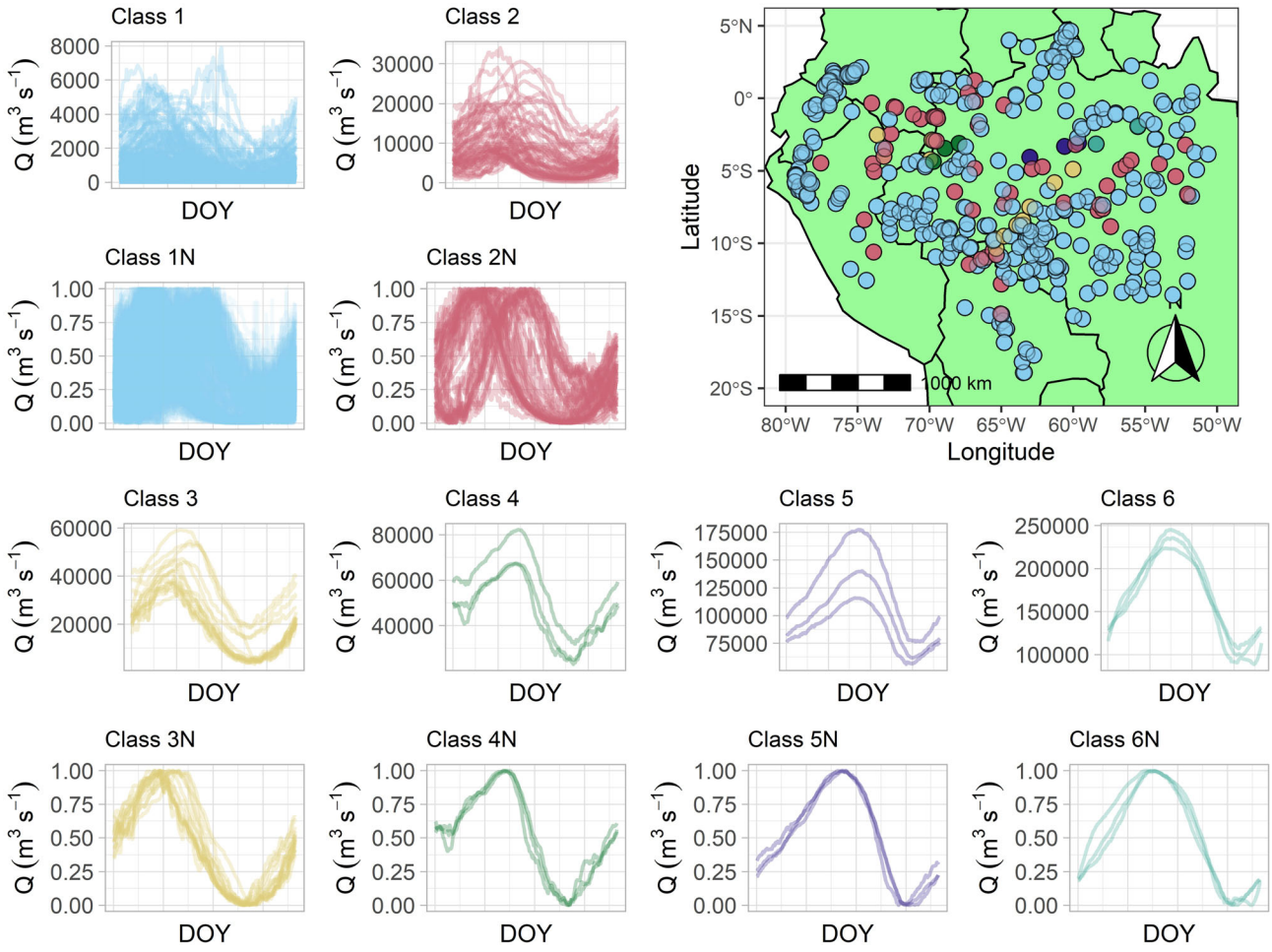

FIGURE 6 Classification results for raw mean annual hydrographs (MAH:Raw). Normalized hydrographs for each class are denoted by 'N'. DOY refers to calendar day of the year. Classes are numbered from lowest to highest maximum within-class discharge. Geographically coherent flow regime clusters include class-3 and -5 stations (yellow and purple) across southern and south–central regions, class-4 stations (green) across the north-central Amazon, and class-6 stations (turquoise) along the Amazon/Solimoes mainstem

(Figures 4 and 6) maintained much clearer separation by flow magnitude, but with small membership classes required to accommodate high-flow stations. Although potentially useful for separating large from very large rivers, this division drove large class memberships and low self-similarity for the remaining stations, limiting ecohydrological interpretation without exploring lower-level dendrogram branches. Further descriptions of each method and class and their geographical distributions across the basin are provided in Sections 3.1 and 3.2.

3.1 | IHA-based classification schemes

Using the IHA:All dataset, classes generally represented a continuum from low to high stream order, with the exception of the very large class 4 (Figure 4). With increasing class number, there was also a steady decrease in the average number of reversals (from n = 162 in class 1 to n = 19 in class 6) and decrease in mean elevation. Class-6 stations (n = 6) had the largest average flow magnitudes (10^5 m^3 s^{-1}) and were located along the mainstem of the Amazon (Figure 4). These stations were characterized by high rise rates, low numbers of reversals, and flow maxima around June. Class-5 stations (n = 21) had the next largest average flow magnitude (10^4 m^3 s^{-1}), and were distributed along major tributaries such as the Madeira, Solimoes, and Purus rivers. The emergent properties of relatively smaller rivers were less clear, although some salient features are notable. Classes 2 and 4 were both large and heterogeneous, with low within-group similarity (Table 5). Class 4 had the highest class membership (n = 207) and was distributed widely across the basin, with a wide range of flow magnitudes and seasonal flood timing. This within-class variation is apparent in the cluster dendrogram (Figure S1), which indicates at least two major 'sub-classes'. Class-3 stations (n = 13) had a flow magnitude of approximately 10^4 m^3 s^{-1}, and were mostly distributed across the Peruvian and Bolivian Amazon. Classes 1 (n = 48) and 2 (n = 109) both had lower flow magnitudes (10^2 m^3 s^{-1}) and were differentiated from each other by hydrograph timing (maxima in June versus April, respectively) and flashiness (e.g. more reversals in class 1). Class-2 stations were distributed along higher-elevation regions of the south-western and northern Amazon, whereas class-1 stations were concentrated in

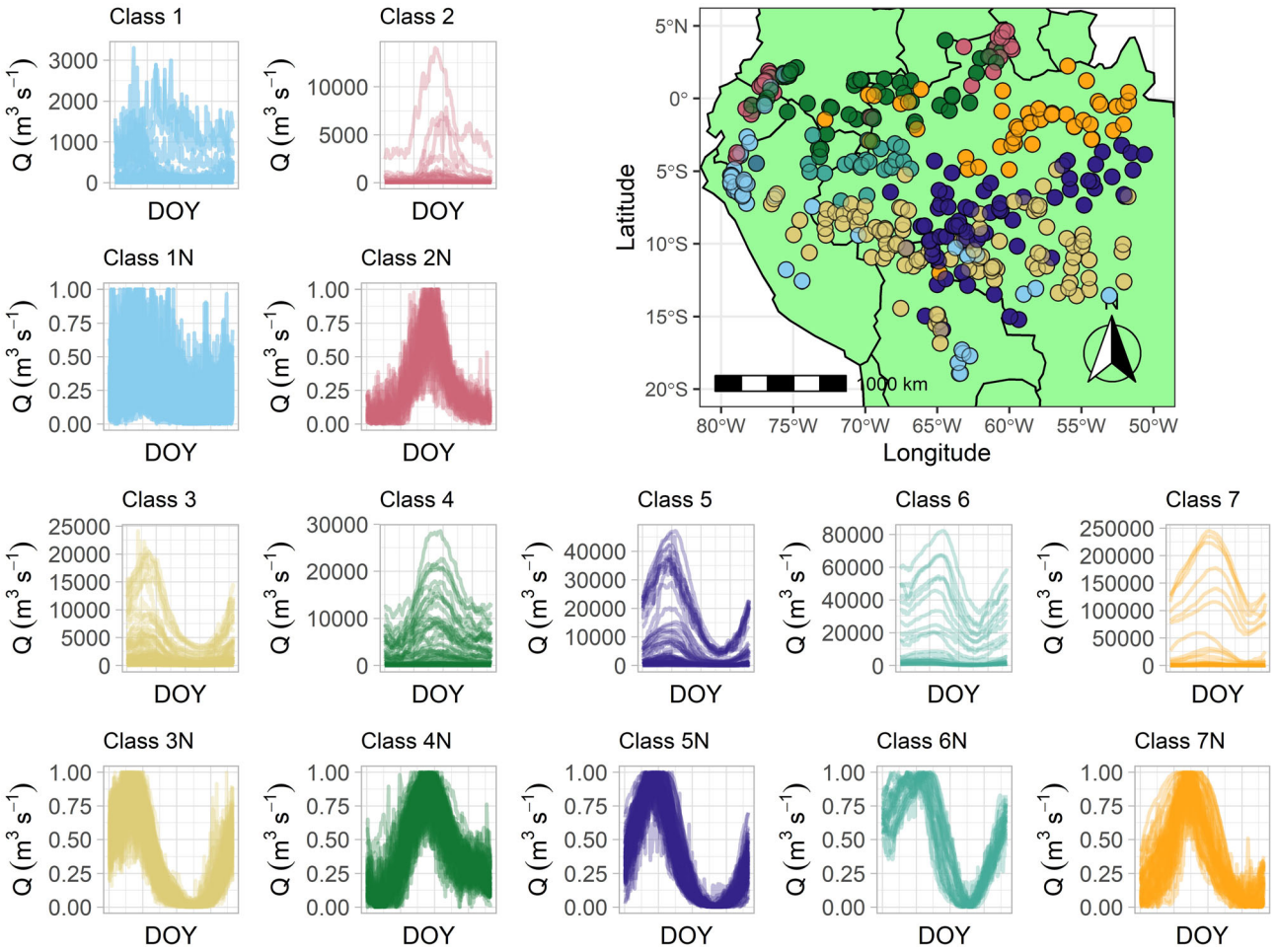

FIGURE 7 Classification results for normalized mean annual hydrographs (MAH:Normalized). Normalized hydrographs for each class are denoted by 'N'. DOY refers to calendar day of the year. Classes are numbered from lowest to highest maximum within-class discharge. Geographically coherent flow regime clusters include class-1 and -2 stations (light blue and red) in the highest-elevation regions ringing the basin, class-3 and -5 stations (yellow and dark blue) across southern and south–central regions, class-4 stations (green) across the northern Amazon, and class-6 and -7 stations (turquoise and orange) along the Amazon/Solimoes mainstem and north–central region

the highest-elevation regions of the Colombian and Ecuadorian Amazon.

Excluding flow magnitude parameters from the IHA-based analysis (IHA:MI) yielded a more even distribution of stations across classes (Table 5). As with IHA:All, the average class elevation decreased and stream order generally increased across classes, although differentiation in seasonality among classes was more apparent (Figure 5). Class 6 (n = 27) retained the large mainstem Amazon stations from IHA:All but added stations along the mainstems of major tributaries (Madeira, Tapajos, and Solimoes), the (relatively) lower flow magnitudes of which (10^4 versus 10^5 m^3 s^{-1}) had separated these stations in the IHA:All analysis. In addition to high flow magnitudes (10^4 m^3 s^{-1}), these stations had high rise rates and low numbers of reversals. IHA:MI classes 3, 4, and 5 all had relatively similar average flow magnitudes (10^3 m^3 s^{-1}), high NCC values, and spatially coherent distributions. IHA:MI class-3 stations (n = 9) across Peruvian and Bolivian upland rivers had high rise rates and relatively flashy behaviour, resembling class 3 in the IHA:All analysis. Class-4 stations (n = 46) were characterized by a mid-annual wet season and a relatively low number of reversals and were clustered conspicuously across the northern Amazon. Classes 2 and 5 had the highest number of stations (n = 126 and 149, respectively), with stations distributed across the entire basin (Figure 5). Class-5 stations shared a generally sinusoidal MAH, whereas class-2 stations were flashier and more heterogeneous. IHA:MI class-1 stations (n = 47) overlapped almost completely with IHA:All class-1 stations (n = 48), representing the highest-elevation, low-magnitude, flashy rivers of the Colombian and Ecuadorian Amazon.

3.2 | Hydrograph-based classification schemes

Classification using daily values of the mean annual hydrograph (MAH:Raw) was overwhelmed by the enormous range in flow magnitudes across the dataset, leading to the largest disparity in class number (from three to 323 stations; Table 5). The three highest-

TABLE 5 Mean statistics for all classifications

	Class	1	2	3	4	5	6
IHA:All	No. of stations	48	109	13	207	21	6
	Jaccard index	0.57	0.42	0.61	0.66	0.70	0.82
	NCC (mean = 0.49)	0.49	0.58	0.66	0.40	0.92	0.98
	Stream order	4.0	4.8	7.2	5.3	7.0	9.7
	Elevation (m a.s.l.)	1,172	725	253	157	83	14
	Flow magnitude ($m^3\ s^{-1}$)	218	238	5,677	2,145	26,491	138,025
	Date flow minima	105	243	245	226	269	315
	Date flow maxima	180	85	63	111	105	160
	Rise rate	53.0	37.1	503	52.1	386	633
	No. of reversals	162	102	106	54	50	19
	Class	**1**	**2**	**3**	**4**	**5**	**6**
IHA:MI	No. of stations	47	149	9	46	126	27
	Jaccard index	0.66	0.49	0.55	0.76	0.62	0.67
	NCC (mean = 0.65)	0.62	0.43	0.70	0.88	0.82	0.72
	Stream order	4.0	4.8	7.4	5.5	5.3	8.0
	Elevation (m a.s.l.)	1,157	573	276	172	167	72
	Flow magnitude ($m^3\ s^{-1}$)	223	470	4,923	3,571	2,330	50,227
	Date flow minima	101	256	265	37	274	278
	Date flow maxima	176	94	62	175	86	111
	Rise rate	54	38	583	103	42	456
	No. of reversals	162	93	116	65	46	46
	Class	**1**	**2**	**3**	**4**	**5**	**6**
MAH:Raw	No. of stations	323	57	15	3	3	3
	Jaccard index	0.96	0.74	0.77	0.71	0.91	0.92
	NCC (mean = 0.35)	0.30	0.39	0.94	0.97	0.99	0.98
	Stream order	4.8	6.3	7.3	9.0	9.3	10.0
	Elevation (m a.s.l.)	508	127	84	73	22	7
	Flow magnitude ($m^3\ s^{-1}$)	478	7,817	23,977	50,342	105,762	170,288
	Date flow minima	220	196	270	267	312	317
	Date flow maxima	108	121	101	127	169	152
	Rise rate	39.9	206	402	456	433	834
	No. of reversals	89	48	56	24	9	28
	Class	**1**	**2**	**3**	**4**	**5**	**6**	**7**
MAH:Normalized	No. of stations	52	33	102	60	83	26	48
	Jaccard index	0.66	0.68	0.67	0.81	0.73	0.75	0.88
	NCC (mean = 0.83)	0.40	0.81	0.93	0.83	0.95	0.90	0.86
	Stream order	4.7	4.5	5.3	4.9	5.5	5.7	5.6
	Elevation (m a.s.l.)	1,384	1,295	210	324	131	110	79
	Flow magnitude ($m^3\ s^{-1}$)	131	494	1,403	2,922	3,862	13,448	19,312
	Date flow minima	252	84	258	66	278	259	271
	Date flow maxima	109	180	60	178	87	96	140
	Rise rate	38.3	51.6	88.1	89.7	96.3	165	115
	No. of reversals	119	134	76	97	53	44	59

Note: NCC = normalized cross-correlation. Flow magnitude refers to the mean value of median annualized hydrographs within each class. Indicators of hydrologic alteration (IHA): IHA:All, classification including all parameters; IHA:MI, flow magnitude-independent classification; MAH:Raw, median annualized hydrograph raw classification; MAH:Normalized, median annualized hydrograph normalized classification. Stream order determined according to Pfafstetter (1989).

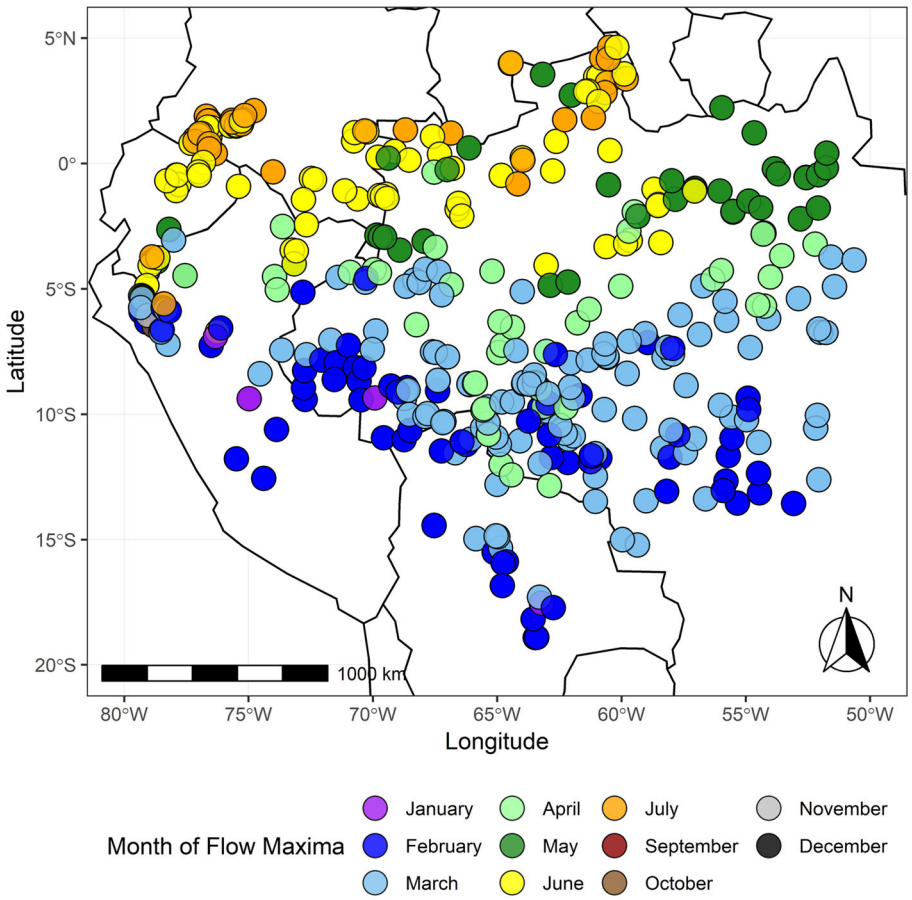

FIGURE 8 Timing of flow maxima across all stations in the study

magnitude flow classes (10^4–10^5 m^3 s^{-1}) each had only three members, representing high-order, lowland stations (Figure 6). Among these groups, class differentiation was driven by differences in flow magnitude (increasing with distance downstream), number of reversals (lowest for mid-reach class-5 stations), and flood-pulse timing (earliest for class-4 stations near the Brazil–Colombia–Peru border). Class-3 stations (n = 15) also had relatively large flow magnitudes (10^4 m^3 s^{-1}) but with earlier flow maxima than classes 4–6 and were located primarily on the Madeira River (Figure 6). Classes 1 (n = 57) and 2 (n = 323) were distributed across the Amazon and represented a wide variety of flow regime characteristics, including early and mid-annual wet seasons, a range of (relatively low) flow magnitudes and rise rates, and (relatively high) number of reversals. Additional, unclassified flow regime structure within these classes is apparent in the 'noisy' MAHs in Figure 6, low NCC values (Table 5), and MAH:Raw dendrogram (Figure S3).

In sharp contrast, classification using the MAH:Normalized dataset produced seven classes with the most even station distribution (Table 5). Although classes were distributed across a clear elevation gradient, stream order did not vary correspondingly. This suggests less scale-dependent station clustering, with variance in timing and rate of change more strongly driving classification. For example, wet/dry-season timing varied coherently among classes, with class 3 (flow maxima/minima in February/September), class 5 (flow maxima/minima in March/October), and class 6 (flow maxima/minima in April/September) representing earlier wet seasons. Later wet-season onset was associated with class 1 (flow maxima/minima in late April/September), class 7 (flow maxima/minima in May/September), class 4 (flow maxima/minima in June/early March), and class 2 (flow maxima/minima in May/September). No other method yielded such clear differences in flow timing among classes. Class-7 stations (n = 48) had the largest average flow magnitudes (10^4 m^3 s^{-1}) and were situated both along the Amazon mainstem as well as lower-order rivers in the northern and north-eastern Amazon (Figure 7). Class-6 stations (n = 26) were differentiated by an earlier flood peak, the highest rise rates, and the lowest number of reversals, although classes 5–7 were all relatively 'un-flashy'. Class-6 stations were located in a tight cluster in the west-central basin, largely on the Jutai, Solimoes, Jurua, and Itui rivers. Classes 3–5 shared a similar order of flow magnitude (10^3 m^3 s^{-1}), but classes 3 (n = 102) and 5 (n = 83) had an early-season flood peak and class-4 stations (n = 60) had later flow maxima. Class-3 stations were located across a broad swathe of the southern Amazon and partly overlapped with class-5 stations in the Madeira basin. Class-4 stations (n = 60) were consistently located on mid-elevation rivers in the northern Amazon (Figure 5). Classes 1 and 2 had the smallest average discharge (10^2 m^3 s^{-1}) and highest number of reversals. Class-2 hydrographs shared a coherent mid-season peak, whereas class-1 stations were more heterogeneous. These high-elevation stations ring the basin, with class-2 stations in Ecuador and northern Brazil and with class-1 stations in Peru, Bolivia,

and southern Brazil (Figure 7). Table S2 provides an overview of differences among approaches and resulting classes.

3.3 | Comparison with GloRiC

The spatial distribution of rivers based on their assigned GloRiC class is shown in Figure 9. Across 15 potential combinations of flow magnitude and variability groups, the 404 stations analysed here corresponded to 12 GloRiC classes. GloRiC station classification aligned strongly with stream order, with stations recording very high flow magnitudes and medium-to-high flow variation located at outlets of the Madeira, Solimoes, Tapajos, Negro, and Caquetá rivers. Stations with very low flow magnitudes were generally located in the Andean Amazon, corresponding to class-1 and -2 stations within the framework. Overall, the categorical, log-based streamflow classifications from GloRiC yielded a relatively even station membership across classes (Figures S7–S9; Table S3), although with substantial within-group variation in MAH. For the 12 classes in the GloRiC database, within-class NCC values ranged from 0.29 to 0.99, and the station-weighted average NCC was 0.42, considerably lower than the flow magnitude-independent methods, despite having twice as many classes. Notably, the GloRiC classes did not show apparent trends in timing, which is reasonable given that intra-annual temporal parameters were excluded from the classification. However, the combination of log-based flow magnitude and streamflow variability thresholds from GloRiC was successful in identifying rivers with unique hydrological behaviour. Specifically, the Paraiso and Abapo stations in the Bolivian Amazon (identified as class 1 or 2 in this analysis across all methods) were the only stations that corresponded to the medium flow magnitude/very high flow variance class (Figure S7), thus identifying two rivers that are surprisingly flashy given their high flow magnitudes.

4 | DISCUSSION

To the best of our knowledge, this study represents the first effort to classify Amazonian rivers using observed streamflow data. Our analysis characterized patterns in streamflow variation to capture ecologically relevant flow regime classes across the Amazon basin, using a classification framework that distinguished flow regime classes according to streamflow magnitude (in flow magnitude-inclusive approaches), frequency, timing, and rate of change to produce classes with the highest possible within-class hydrological similarity and between-class difference. This study highlights the wide range and geographical distribution of streamflow characteristics across the vast Amazon basin, describes relationships among various streamflow components, and connects river dynamics to regional and global climatological cycles. Building from a set of 404 flow gauging stations, this inductive classification yielded a parsimonious set of six and seven hydrological classes using a flow magnitude-independent subset of IHA parameters and normalized mean annual hydrographs, respectively. For all methods, class membership was strongly associated with flow elements related to timing, frequency, and rate of

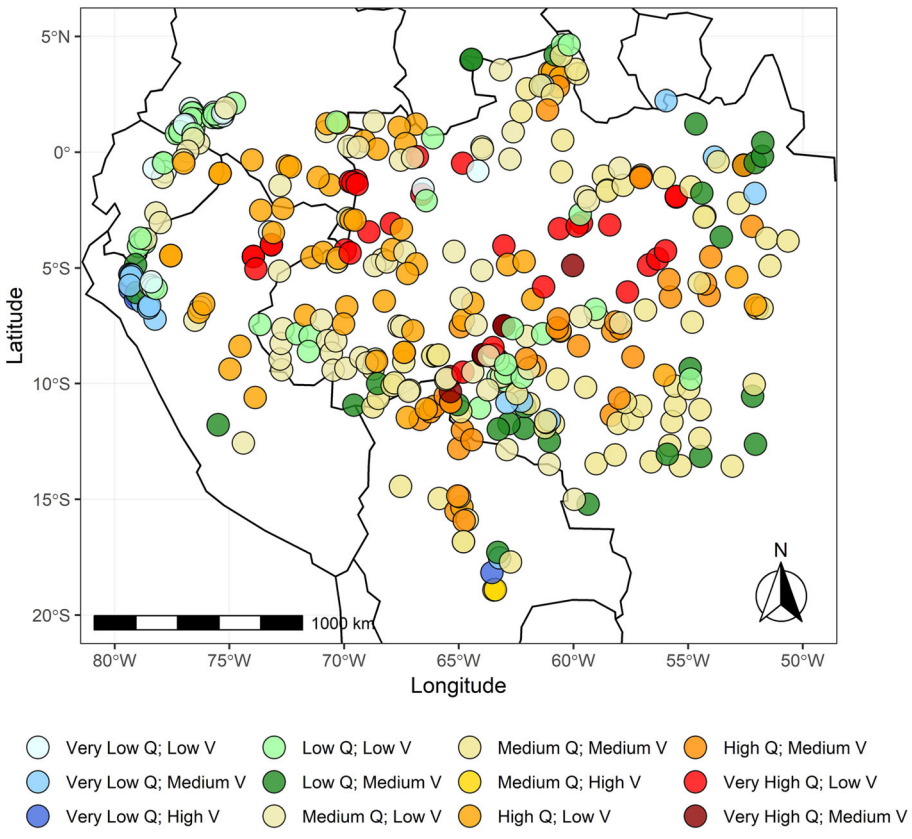

FIGURE 9 Global River Classification (GloRiC) hydrological classification for observed streamflow stations. The GloRiC framework includes 15 distinct hydrological classes with five levels of flow magnitude (*Q*), very low (0.1–10 $m^3 s^{-1}$), low (10–100 $m^3 s^{-1}$), medium (100–1,000 $m^3 s^{-1}$), high (>1,000–10,000 $m^3 s^{-1}$), and very high (> 10,000 $m^3 s^{-1}$), and three levels of flow variability index (*V*), low ($V < 2$), medium ($2 < V < 3$), and high ($V > 3$) (Ouellet-Dallaire et al., 2019). Variability is defined as the maximum of the long-term average monthly discharge divided by the long-term average discharge. Modelled discharge data in GloRiC come from the global freshwater model WaterGAP (Döll et al., 2003). Flow regime clusters are strongly aligned with stream order (e.g. stations with very high flow magnitude and medium/high flow variation located along the mainstems of the Madeira, Solimoes, Tapajos, Negro, and Caquetá rivers)

change. Although no geographical coordinates or other proximity metrics were included in the classification, spatial coherence was apparent across most classes in all methods, probably driven by inherently hierarchical relationships among stream order, latitude, and elevation that give rise to the flow regime (Snelder, Biggs, & Woods, 2005).

Overall, these results allow for the exploration of how ecologically relevant streamflow characteristics vary across the Amazon and demonstrate how the choice of input data drives clustering results and subsequent ecological interpretation. For example, in the IHA:MI and MAH:Normalized classifications (Figures 4 and 6), flow regime characteristics related to timing and flashiness emerged as major drivers of flow regime differentiation. As these classifications were very strongly associated with hydrograph shape, specific seasonal signatures potentially related to fish migration and spawning cues (Cañas & Pine, 2011; Jiménez-Segura, Palacio, & Leite, 2010) were apparent among classes. In contrast, for the two methods that retained flow magnitude (IHA:All and MAH:Raw; Figures 4 and 5), classes were clearly aligned from low to high flow magnitude, representing an upstream-to-downstream (i.e. low-to-high stream order) gradient strongly associated with habitat types and ecosystem functioning (Vannote, Minshall, Cummins, Sedell, & Cushing, 1980). Below, we discuss the ecological significance of these flow regime classifications, compare them with existing classifications, suggest how these results can be used in future river research, and to guide freshwater management and conservation decisions, and briefly summarize methodological considerations of the classification approach.

4.1 | The ecohydrology of Amazonian flow regimes

Flow regimes across the Amazon support a remarkable diversity of aquatic ecosystem structure, function, and services (Anderson et al., 2018; Castello & Macedo, 2016). It is thus perhaps surprising that a limited set of six or seven flow regime classes could be used to describe ecohydrological variation across this vast region. Although every river reach – and indeed each year of flow within each reach – is likely to contain unique attributes along a gradient of streamflow behaviour, this parsimonious set of classes was statistically supported for flow magnitude-independent datasets. The further splitting of classes into more highly resolved groups is possible by applying a lower clustering threshold. Following from the large body of work on flow regime characteristics (Palmer & Ruhi, 2019; Poff et al., 2010; Richter et al., 1996), the salient organizing features of the flow classes identified here include flow magnitude, duration, timing, frequency, and rate of change, in line with the original 'natural flow regime' concept (Poff et al., 1997). These attributes characterize flow regime behaviour and have been directly linked to aquatic species evolution (de Assis & Wittmann, 2011) and ecological response to disturbance (Leigh, Stewart-Koster, Sheldon, & Burford, 2012). Whereas both IHA and MAH approaches reflect these five flow regime features, IHA-based analyses are useful for directly connecting the flow metrics that strongly influenced our classifications (Figures S5 and S6) with established or hypothesized ecological relationships in the Amazon (Table 6).

The strong influence of flow magnitude on Amazon ecohydrology follows intuitively from the river continuum concept (RCC). The RCC connects gradients in physical properties to characteristic streamflow properties associated with a gradient of ecological processes (Vannote et al., 1980), including maintaining riparian vegetation, habitat availability for aquatic organisms, food and water availability for fauna, predictability of water availability, access to nesting sites, and influence on abiotic factors (Castello & Macedo, 2016). Discharge magnitude is a key component of the flood pulse and is associated with lateral and longitudinal connectivity through frequency and rate-of-change parameters. The resulting spectrum of flood pulses, from short and unpredictable headwaters to long and predictable high-order rivers (Junk et al., 1989), were captured through both IHA and MAH approaches, with implications for understanding patterns of ecosystem structure and function. Magnitude-inclusive classification schemes were able to differentiate among the largest rivers in the Amazon lowlands (i.e. IHA:All classes 5 and 6 and MAH:Raw classes 4–6). Despite a high degree of seasonality, these very high-order rivers maintain strong base flows all year round and facilitate extremely productive ecosystems (McClain & Naiman, 2008), together with direct human services such as transportation (Domínguez, 2004). Separating these classes when considering the diversity of Amazon flow regimes, even if not statistically supported, may thus be important from both an ecological and a management perspective. For flow magnitude-independent classifications, rivers in IHA:MI classes 4–6 and MAH:Normalized classes 4–7 spanned large flow magnitude gradients and are thus useful for hypothesizing how hydrological alteration will affect rivers with similar flow regime 'shapes' along large discharge and spatial gradients. Although flow magnitude-independent approaches were better for identifying shared flow regime characteristics in low-order streams (classes 1 and 2), in all cases further splitting would support a more localized interpretation of streamflow variation.

Strongly tied to mean flow magnitude, extreme flow parameters quantify discharge maxima and minima over multiple timescales (Tables 3 and 4). Notably, eight of the 10 strongest drivers of PCA variation for the IHA:All dataset were extreme flow metrics (1-, 3-, 7-, 30-, and 90-day maxima, small flood peak, and May/January low flows; Figure S5). It should be noted, however, that flow extremes are often correlated with mean flow (Olden & Poff, 2003), especially for high-discharge rivers. Indeed, flow extremes associated with IHA:All classes 1–6 varied in concert with overall mean flows (e.g. 90-day maximum and mean flows in Table 5). Ecologically, extreme events are directly linked to floodplain inundation and the evolution of communities adapted to predictable flooding (Parolin, 2012). River–floodplain connectivity facilitates the life cycles of hundreds of fish species (Anderson et al., 2018; Barthem et al., 2017; Correa & Winemiller, 2018; Miranda-Chumacero, Álvarez, Luna, Wallace, & Painter, 2015), migratory fish passage, and speciation at the whole-basin scale (Lowe-McConnell, 2011; Oberdorff et al., 2019). Extreme high and low flows are also linked to sediment erosion and deposition,

TABLE 6 Ecologically relevant flow metrics across the Amazon basin

Metric	Significance	Ecological relevance
90-day maximum*	Average maximum magnitude over 90-day (seasonal) period	Shifts in flow maxima over a seasonal time interval, through drought and flooding conditions, are linked to the mortality of trees in the Amazon and the resulting changes in forest structure and function (Nepstad, Tohver, David, Moutinho, & Cardinot, 2007), soil moisture stress, and anaerobic stress (Parolin, 2012)
30-day maximum*	Average maximum magnitude over 30-day (monthly) period	Roughly corresponds to the monthly interval of river peak flows, aligning with rates of sediment and nutrient delivery (Dunne et al., 1998), and increased spawning of catfishes (Siluriformes: Pimelodidae) along Andean–Amazon gradient (Cañas & Pine, 2011)
Small flood peak*	Average magnitude of stream flow during small floods	Migration and spawning cues for migratory fish, including the catfish family Siluriformes: Pimelodidae (Cañas & Pine, 2011), connecting lentic and lotic habitats and facilitating the movement of *Arapaima gigas* (Castello, 2008)
Rise rate**	Average of differences in streamflow increases between consecutive days	Rising water levels in the Middle Solimões River act as 'a natural barrier' between floodplain lakes and the Solimões River, thereby structuring fish passage and assemblage (Sousa & Freitas, 2008). Work in temperate basins provides evidence of fish stranding, destabilization of sediment accumulation, disruption of riparian plant and animal life cycles (Richter et al., 1996), and the failed establishment and recruitment of seedlings (Renöfält, Jansson, & Nilsson, 2010)
No. of reversals**	Average number of reversals between rising and falling daily flows	Studies in temperate basins provide evidence of fish stranding, destabilization of sediment accumulation, disruption of riparian plant and animal life cycles (Richter et al., 1996), weakening of river banks, and loss of vegetation (Renöfält et al., 2010). These ecohydrological relationships may also be observed in tropical basins and further studies in the Andean–Amazon gradient are needed
High flow rise and fall rates**	Average rise/fall rates during high flow events	High flow rise and fall rates have been included in environmental flow assessments, although as yet no studies have been found that have connected high flow rise and fall rates with an ecological response in the Amazon
High pulse count**	Average number of high pulses	Research in temperate basins relates a high pulse count to soil moisture stress, anaerobic stress, the availability of floodplain habitat, and nutrient and organic-matter exchange (Richter et al., 1996), and identifies decreased high pulse count as a driver of the long-term dehydration of riparian habitat and dominance of terrestrial ecosystems (Poff & Zimmerman, 2010). The study of such relationships in the Andean-Amazon and other tropical basins is needed

Note: These parameters were the strongest drivers of streamflow classification from the IHA:All (*) and IHA:MI (**) classifications.

forming thousands of kilometres of river habitat (Constantine, Dunne, Ahmed, Legleiter, & Lazarus, 2014), especially in high-discharge white-water rivers (Espinoza Villar et al., 2013), such as the Madeira, Solimoes, Purus, and Caquetá-Japura. Maintenance of these extreme highs and lows, and the longitudinal and lateral connectivity that they support, is thus fundamental for conservation and biodiversity protection. Critically, the connectivity in some basins (e.g. Beni, Mamore, Marañón, and Ucayali) is vulnerable to alteration from existing and proposed dams (Anderson et al., 2018; Finer & Jenkins, 2012), posing a risk to river biodiversity and highlighting the importance of acknowledging flow extremes in Andes–Amazon conservation efforts (Farias et al., 2019).

We found streamflow timing (i.e. wet/dry-season onset) to be one of the most differentiable and interpretable aspects of flow regime classification across the Amazon, especially for the two flow magnitude-independent approaches (Figures 5 and 7; Table 5). In particular, classes 2–7 in the MAH:Normalized classification scheme all had relatively similar MAH shapes but were differentiated by wet/dry-season timing (among other flow attributes). The bimodal distribution of seasonality (assessed through date of flow maxima) on either side of the mainstem (Figure 8) is attributed to latitude, high rainforest evapotranspiration rates ('recycling of precipitation'), and global climate patterns, with additional effects from basin biophysical features such as slope, land cover, soils, and river–floodplain interactions (Fleischmann et al., 2016). The approximately 6,000-m elevation gradient of the basin also plays a strong role in driving flow timing, with higher-elevation rivers in the Peruvian and Ecuadorian Amazon more heavily influenced by sporadic storm events compared with strongly seasonal precipitation signals (e.g. contrast class 1 with all other classes for MAH:Normalized in Figure 7). Streamflow timing is linked to rates of biogeochemical cycling, riparian productivity, and the spawning and migration of myriad fish species (Yarnell et al., 2020). For example, floodplain cichlids (*Symphysodon* spp.) generally spawn at the onset of the wet season following flow and water-quality cues (Crampton, 2008). Directional changes in streamflow timing in the Amazon may be driven by climate change (Arias et al., 2020, Guimberteau et al., 2013) or direct flow manipulation (Timpe & Kaplan 2017), and if they occur more quickly than species can adapt, can lead to local species extinction (Hwan & Holmes, 2020).

The frequency of high and low pulses drives the exchange of materials between the river and the floodplain, structuring biotic

relationships along the entire river (Junk et al., 1989). High flow frequency and extreme low-flow frequency were influential in both the IHA:All and IHA:MI classifications (Figures S5 and S6). Across methods, the lowest extreme low-flow frequencies and highest high-flow frequencies were bookended by MAH:Raw class 1 and IHA:MI class 6 (Data S2), representing the overall low- to high-flow gradient. The maintenance of these hydrological indicators is tied to the maintenance of channel geomorphology, area of floodplain habitat, and food-web complexity (Hayes et al., 2018). For example, many of the Amazon's large catfish (Siluriformes: Pimelodidae) rely on the predictable frequency (and timing) of flow events for spawning and the transport of larvae (Cañas & Pine, 2011). The flood-pulse concept (Junk et al., 1989) asserts that low-order streams such as those in the high Andes (e.g. IHA:MI class 1; Figure 5) are characterized by short and generally unpredictable flood pulses, with species adapted to survive quickly changing riparian zones (Godoy, Petts, & Salo, 1999; Larson, 2019; Parolin, 2012; Polato et al., 2018). Conversely, higher-order streams (e.g. those in IHA:All classes 5 and 6; Figure 4) aggregate in incoming tributaries, minimizing the influence of precipitation and displaying more predictable interannual flood frequencies. The transition from high Andes and cordillera ecosystems to piedmont (piedmonte) and floodplain (llanura) ecosystems is thus accompanied by a decreasing flood-pulse frequency and increasing streamflow predictability; this trend was generally well captured by three of the four classification approaches (IHA:All, IHA:MI, and MAH:Normalized; Figures 4, 5, and 7).

The rate and frequency of hydrological changes reflect the day-to-day hydrological predictability experienced by aquatic flora and fauna, and are quantified by rise rates, fall rates, and the number of reversals (Table 3). For flow magnitude-independent approaches, river classification was structured by rate-of-change and frequency parameters (in IHA:MI) and by frequency and timing (in MAH:Normalized). Reversals in particular were a useful indicator that helped differentiate classes along a gradient from 'flashier' upland streams to 'smoother' floodplain rivers, to which aquatic flora and fauna have adapted their unique life-cycle histories. Ecologically, less flashy rivers with more predictable dry-season base flows (e.g. IHA:MI classes 5 and 6) minimize the drought stress that is faced by organisms in flashier, upland rivers (i.e. IHA:MI classes 1 and 2). As drought risk in the region intensifies (Marengo & Espinoza, 2016), more studies are needed to determine the ecological effects of drought on susceptible streams in the Andean Amazon; recent studies in Andean headwater streams demonstrate how steep topographical gradients exert a significant role in structuring functional, taxonomic, and phylogenetic community composition (Larson, 2019).

4.2 | Alignment with existing Amazon classifications

By emphasizing the flow regime, this classification complements global-scale environmental classifications such as the Freshwater Ecoregions of the World (FEOW; Abell et al., 2008). FEOW contains 11 ecoregions in the topographical Amazon (Amazonas Guianan Shield, Rio Negro, Western Amazon Piedmont, Ucayali Piedmont, High Andes, Mamore, Guapore, Madeira Brazilian Shield, Tapajos-Juruena, and Xingu) and presents several ecoregions that overlap with our hydrological classes (e.g. Amazonas Lowlands, corresponding to large floodplain rivers in higher-order classes across methods; Figures 4–7). Ecologically, these river basins contain seasonally inundated and flooded forests (várzea and igapó), swamp forests, terra firme forests, and floating meadows (Abell et al., 2008). Classes 1 and 2 in both IHA classifications correspond well to Andes–Amazon rivers (FEOW:Amazonas High Andes), including the Caquetá, Putomayo, Napo, Beni, and Marañón. These rivers are marked by fast-flowing streams with much lower base flows. The Andes are considered one of the most diverse habitats on earth, with ecoregions subdivided into submontane forest (700–2,000 m a.s.l.), montane forest (2,000–2,500 m a.s.l.), cloud forest (2,500–3,500 m a.s.l.), and puna (3,500+ m a.s.l.) (Abell et al., 2008). Although none of our classification schemes fully captured differences across this elevation gradient (partly owing to the availability of flow data), the MAH:Normalized approach best identified unique flow regime characteristics for high-elevation rivers (Figure 7).

Our classification also complements the GloRiC (Ouellet-Dallaire et al., 2019), which used modelled hydrological data to classify flow regimes. The observed discharge data presented in this study provides an opportunity to extract signatures that may not be as easily extracted or validated in modelled data. It should be noted that GloRiC authors selected magnitude and variation as driving features of flow variation after analysing hydrological variation at the global scale. This intentional exclusion of seasonality at least partly accounts for lower within-class MAH similarity for GloRiC classes (i.e. lower NCC values). A more informative characterization of GloRiC classes is seen in Figure S7, indicating the strong correspondence of observed median discharge to GloRiC classes. Our flow magnitude-inclusive schemes generally corresponded to GloRiC classes (Figures 4–6 and S9), and flow magnitude-independent schemes revealed additional variability in frequency and rate-of-change parameters (Figures 5 and 7). In short, our results accord with the GloRiC characterization of magnitude across the basin and add further details about variance in other ecologically relevant flow metrics (timing, frequency, and rate of change).

4.3 | Application and utility of derived flow classifications

This analysis supports the prioritization of aquatic conservation and monitoring efforts across the Amazon by synthesizing the spatio-temporal availability of Amazonian flow data, quantifying regions of shared and divergent flow regime characteristics and identifying major drivers of flow regime classes. The monitoring and forecasting of streamflow dynamics across the entire basin has been identified as a primary research and management need (Junk, 2013), and the database accompanying this article provides observed discharge

time series, IHA/EFC metrics, hydrographs, additional metadata (Data S2), and classifications for 404 Amazon rivers, publicly available and accessible through HydroShare (https://www.hydroshare.org). These results also improve our understanding of the natural flow regime at the whole-basin scale, supporting the development of more regionally specific analyses of environmental flows. Notably, this effort accomplishes the first two steps of the ELOHA framework (Poff et al., 2010): assembling a database of daily streamflow hydrographs across the basin over a period that sufficiently captures climate variability; and classifying river segments using ecologically relevant flow metrics. These two steps set the stage for quantifying hydrological alteration in fluvial systems using a set of streamflow statistics strongly connected to ecological function (Poff et al. 2010).

Although the development of river- or reach-specific environmental flows programmes require more site-specific analysis, the classifications produced here revealed generally cohesive spatial distributions of classes, driven by magnitude and duration parameters in flow magnitude-inclusive schemes and highlighting variation in timing, frequency, and rate-of-change parameters for flow magnitude-independent approaches. In particular, the classifications presented in this analysis provide four different lenses through which flow alteration may be assessed. IHA:MI or MAH:Normalized classifications enable an analysis of change among stations that vary in flow magnitude yet share similarities in flood frequency, duration, and timing. For example, the range of median annual hydrographs for rivers in IHA:MI class 6 and MAH:Normalized classes 6 and 7 connote ecological similarities in the timing and duration of river–floodplain connection across streams of vastly different sizes (Figures 5 and 7; Data S2). Whereas many studies have sought to connect flow magnitude-driven flow metrics and ecological response, less attention has been given to flow magnitude-independent metrics, especially in the Amazon basin. Alternatively, IHA:All and MAH:Raw classifications (Figures 4 and 6) provide relatively straightforward, flow magnitude-driven classes that also reveal other flow magnitude-associated flow regime attributes (e.g. flashiness and base flow).

To be useful in guiding river management in the context of hydrological alteration, data compilation and streamflow classification must be coupled with the development of flow–ecology relationships. There is a growing body of work on the impacts of hydrological alteration from climate (Ahlström et al., 2017; Arnell & Gosling 2013; Davidson et al., 2012), land-use, and land-cover change (Coe, Latrubesse, Ferreira, & Amsler, 2011; D'Almeida et al., 2007; Levy, Lopes, Cohn, Larsen, & Thompson, 2018; Lima et al., 2014), and dams (Timpe & Kaplan, 2017; Valle & Kaplan, 2019), in the Amazon. Given the huge diversity of flora and fauna and ecological dynamics that are linked to freshwater ecosystems, there is a pressing need for additional field studies to determine flow–ecology relationships across natural streamflow regimes in the tropics, including the Andean Amazonian (Wohl et al., 2012), where steep gradients in topography, geology, and soils drive sediment and nutrient transport, ecosystem productivity, and the dependence of migratory species on riverine connectivity (Anderson et al., 2018; Dunne et al., 1998; Encalada et al., 2019; Finer & Jenkins, 2012; McClain & Naiman, 2008). For instance, an ecological integrity index was developed in the Napo River basin to predict river ecological integrity as a function of human disturbance and environmental variables, using known environmental features to assess freshwater ecological functioning (Lessmann et al., 2019). Overall, our analysis suggests that flow magnitude-independent parameters are useful for distinguishing among Amazonian hydrological regimes and thus underscores the need to consider linkages between timing, frequency, and rate-of-change metrics and ecological responses.

The spatial distribution of flow regimes can be used to identify monitoring gaps and parsimoniously select representative field stations for long-term ecological monitoring, where streamflow metrics and climate can be explicitly linked to biotic processes, biogeochemistry, and habitat structure (NEON, 2020). For example, Figure 2 illustrates a paucity of flow monitoring stations in the Ucayali River basin, which shows a very high diversity of flow regimes for its size (e.g. classes 2, 3, 5, and 6 in the IHA:MI; Figure 5). In contrast, the large number of stations on the Madeira River (e.g. class 3 in MAH:Raw) may be useful for other purposes such as infrastructure flood forecasting, but is probably unnecessary for capturing the salient features of Madeira River ecohydrology.

4.4 | Methodological considerations

Intuitively, differences in flow regime classifications were driven by differences in the input data. In deriving one classification from IHA/EFC metrics and another from dimensionless reference hydrographs, the MAH:Normalized classification reflects flow regime variation in Amazon rivers either underestimated or not yet captured by a flow metric, thus revealing variation in flow regimes based on established ecohydrological linkages and objective evaluation of median annualized hydrographs (Lane et al., 2018). Although each method provides useful information about shared variance among stations, removing magnitude in the IHA:MI and MAH:Normalized allowed the emergence of timing, frequency, and rate-of-change parameters that formed cohesive groups (Figures 5 and 7), making these classifications more useful for testing ecological relationships tied to intra-annual variation. A specific benefit of the IHA:MI classification is that it removes the 'wash-out' effect of exponentially distributed flow magnitude across the basin, while still reflecting components indirectly connected to rivers with larger flow magnitudes (frequency and rate of change). In contrast, the MAH:Normalized classification demonstrated the greatest independence from flow magnitude and stream order, and is thus likely to be the most useful for parsing flow regime variation with respect to flashiness, periodicity, and seasonality. Overall, the IHA:All approach may be most useful for holistically integrating multiple hydrological indicators across such a wide area and contextualizing primary components of the flow regime at the basin scale (Figure S5). It is important to reiterate that the two flow magnitude-inclusive approaches did not yield a specific,

statistically supported number of classes, and the selection of six classes presented here was arbitrary; further insight could be gleaned by splitting these flow classes into more highly resolved groups based on their dendrograms. For instance, the further partitioning of IHA:All class 2 into six classes reveals additional shared flow regime characteristics within sub-groups that vary in magnitude, rise rate, and date of flow maxima (Figure S10; Table S4). Generally, all classes (with more than one member) may be resolved into more detailed subclasses to reflect shared and diverging flow characteristics within a larger class at smaller scales.

Both flow magnitude-independent methods extracted ecologically relevant characteristics from the flow regime using a similar number of classes (six versus seven), despite very different data forms (29 ecohydrological parameters versus 365 daily means). MAH:Normalized had higher within-class similarity than IHA:MI (mean NCC of 0.83 versus 0.65), although this is partly explained by the addition of a seventh class. The addition of another class in MAH:Normalized distributed rivers that were in class 1 in IHA:MI to classes 1, 2, and 4 in MAH:Normalized, thereby aggregating more rivers in the central–western Amazon. In comparison with MAH:Normalized, the spatial distribution of IHA:MI seemed to better reflect frequency and rate-of-change parameters indirectly connected to flow magnitude, even though direct flow-magnitude parameters were excluded (Figures 5 and 7). For example, as IHA:MI classes increased in flow magnitude, they exhibited a more consistent positive linear relationship with stream order, compared with MAH:Normalized classes (Table 5), indicating a stronger association with stream order and the retention of parameters indirectly related to flow magnitude. Despite a lack of correspondence with stream order, the MAH:Normalized classification formed spatially coherent classes, most likely attributed to variation in seasonality and number of reversals relative to discharge magnitude, a feature that emerges more clearly in normalized hydrographs (Figure 7).Through aggregation with median annualized hydrographs and using mean IHA summary statistics, this analysis captured characteristic long-term river behaviour but did not explicitly consider rare events. Ecological phenomena such as severe floods or droughts that may redistribute species are thus not associated with these classes as applied. This presents an opportunity for future work in focusing on the spatiotemporal distribution of extreme flow events and their ecohydrological implications.

4.5 | Beyond hydrology

Whereas flow can be regarded as an important ecological variable in regulating aquatic ecosystems, there are multiple spatially variable drivers of ecology at the landscape scale. Notably, the hydrologically derived classes presented here do not correspond to the distribution of geologically derived white-water, black-water, and clear-water rivers (Junk et al., 2011). In evaluating sediment dynamics across the Central Amazon floodplains, Fassoni-Andrade and de Paiva (2019) found high spatial and temporal variability with respect to stream order and basin chemistry. Such information, paired with flow regime behaviour, would be useful for supporting ecological and biogeochemical studies. From an ecological standpoint, Amazonian flow regimes are underpinned by geological differences in river chemistry (i.e. aeration, sediment, and turbidity) that combine with flow characteristics to form strikingly different ecosystems (e.g. igapós and várzea floodplains) directly related to variation in soil fertility, productivity, and richness of fish species (Junk et al., 2011). At several confluence zones, the mixing of waters of vastly different ecosystems enables migrating fish to take advantage of unique habitats. For instance, the mixing of the white-water Pastaza River in the Peruvian Amazon with local black-water rivers and lakes creates an ecosystem with floating mats of vegetation and flooded riparian forests, attracting nearly 300 documented fish species (Anderson et al., 2018).

Although the focus of this analysis was Amazonian rivers, the basin is also widely recognized for large and hydrologically important systems of wetlands, lakes, and floodplains. In contrast to temperate basins, large tropical floodplain systems are characterized by a predictable monomodal flood pulse, where plant and animal species have attuned their life cycles to its seasonal rhythms (Adis & Junk, 2002). Between the Andean Amazon landscape gradients, the same geographical features driving variation in Amazon rivers are likely to result in a unique and varied constellation of water bodies, including glacial lakes, oxbow lakes, floating meadows, and dynamic floodplains (Melack & Hess, 2010).

5 | CONCLUSION

Inductive classifications such as the one presented here strategically organize inherently complex streamflow data, and hydrological classifications can provide insight into trends of ecologically relevant IHA parameters. Inductive classifications are intended for basins with a sufficient coverage of stations. This assumption was largely satisfied in this analysis and highlighted selected basins where additional long-term streamflow monitoring may further refine Amazon flow classification. The wide spatial coverage and availability of long-term streamflow data across the Amazon basin allowed the characterization of baseline flow variation and alteration, and is essential for river monitoring, conservation, and restoration. In the context of human alteration, ascribing both relative and absolute features of flow classes can provide a basis for detecting changes within and across streamflow classes. This enables class-specific analysis of changes in flow regime characteristics that are directly linked to physioclimatic and human regulation of rivers.

Given the rapid pace of human modification of tropical megabasins worldwide (Winemiller et al. 2016), understanding the spatial distribution and predictability of streamflow patterns across basins can provide insight into river functioning at the ecosystem scale and support aquatic conservation and efforts to maintain and restore the natural flow regime (Poff et al., 2010). This concept may be applied in the development of conservation programmes that specifically aim to maintain hydrological diversity. Effective programmes would assess

potential losses in hydrological function or deviations from the natural flow regime and then guide and promote management decisions that ultimately maintain baseline ecological functioning. Future work is needed to determine how climate change, dams, and changes in land use and land cover will affect the wide diversity of natural flow regimes and associated ecosystem structure and function. Accompanying deductive classifications can further inform physical variations that control flow regime variability and extend streamflow characteristics to data-scarce basins. Overall, this comprehensive classification approach can yield available data to assist in the conservation of natural flow regimes given limited financial and organizational resources, further our understanding of flow–ecology relationships, and guide the restoration of altered flows to promote the long-term welfare of freshwater ecosystems across the Amazon basin.

ACKNOWLEDGEMENTS

This material is based upon work supported by the National Science Foundation Graduate Research Fellowship under grant no. DGE-1842473. Support for this work was also provided by the Living Andean Rivers project, with generous funding from The MacArthur Foundation under grant agreement #16-1607-151 to E.P.A. Both X.Z.-R. and S.T. gratefully acknowledge financial support provided by Escuela Politécnica Nacional through research project PIMI-17-04. All authors thank Drs Fabrice Duponchelle and Gérard Cochonneau for assistance in gaining access to SO HYBAM streamflow data. All the authors also thank three anonymous reviewers for their helpful and constructive feedback. S.S. and D.K. are grateful to Drs Nathan Reaver, Trey Crouch, and Elliott White for providing thoughtful and constructive feedback, as well as Pamela Senesi, Shaun Taylor, and Christine Swanson for assistance with data processing.

CONFLICT OF INTEREST

The authors declare that there are no conflicts of interest associated with this work.

OPEN RESEARCH BADGES

This article has earned an Open Data badge for making publicly available the digitally-shareable data necessary to reproduce the reported results. The data are available at https://www.hydroshare.org/resource/b43116c378da441cb48b14478d838124/.

ORCID

Sharmin F. Siddiqui https://orcid.org/0000-0002-5061-7506
Xavier Zapata-Rios https://orcid.org/0000-0002-8458-8598
Sandra Torres-Paguay https://orcid.org/0000-0003-3581-9086
Andrea C. Encalada https://orcid.org/0000-0003-2497-6086
Elizabeth P. Anderson https://orcid.org/0000-0003-4641-5810
Carolina Rodrigues da Costa Doria https://orcid.org/0000-0003-1638-0063
David A. Kaplan https://orcid.org/0000-0002-0103-0928

REFERENCES

Abell, R., Thieme, M. L., Revenga, C., Bryer, M., Kottelat, M., Bogutskaya, N., … Petry, P. (2008). Freshwater ecoregions of the world: A new map of biogeographic units for freshwater biodiversity conservation. *Bioscience*, *58*, 403–414. https://doi.org/10.1641/b580507

Adis, J., & Junk, W. J. (2002). Terrestrial invertebrates inhabiting lowland river floodplains of Central Amazonia and Central Europe: A review. *Freshwater Biology*, *47*, 711–731. https://doi.org/10.1046/j.1365-2427.2002.00892.x

Ahlström, A., Canadell, J. G., Schurgers, G., Wu, M., Berry, J. A., Guan, K., & Jackson, R. B. (2017). Hydrologic resilience and Amazon productivity. *Nature Communications*, *8*, 387. https://doi.org/10.1038/s41467-017-00306-z

Anderson, E. P., Jackson, S., Tharme, R. E., Douglas, M., Flotemersch, J. E., Zwarteveen, M., … Arthington, A. H. (2019). Understanding rivers and their social relations: A critical step to advance environmental water management. *Water*, *6*, e1381. https://doi.org/10.1002/wat2.1381

Anderson, E. P., Jenkins, C. N., Heilpern, S., Maldonado-Ocampo, J. A., Carvajal-Vallejos, F. M., Encalada, A. C., & Tedesco, P. A. (2018). Fragmentation of Andes-to-Amazon connectivity by hydropower dams. *Science Advances*, *4*, e1642. https://doi.org/10.1126/sciadv.aao1642

Anderson, E. P., Osborne, T., Maldonado-Ocampo, J. A., Mills-Novoa, M., Castello, L., Montoya, M., … Jenkins, C. N. (2019). Energy development reveals blind spots for ecosystem conservation in the Amazon Basin. *Frontiers in Ecology and the Environment*, *17*, 521–529. https://doi.org/10.1002/fee.2114

ANEEL: Agência Nacional de Energia Elétrica. (2019). Retrieved from https://www.aneel.gov.br/

Arias, M. E., Farinosi, F., Lee, E., Livino, A., Briscoe, J., & Moorcroft, P. R. (2020). Impacts of climate change and deforestation on hydropower planning in the Brazilian Amazon. *Nature Sustainability*, *3*, 430–436. https://doi.org/10.1038/s41893-020-0492-y

Arnell, N. W., & Gosling, S. N. (2013). The impacts of climate change on river flow regimes at the global scale. *Journal of Hydrology*, *486*, 351–364. https://doi.org/10.1016/j.jhydrol.2013.02.010

Auerbach, D. A., Buchanan, B. P., Alexiades, A. V., Anderson, E. P., Encalada, A. C., Larson, E. I., & Flecker, A. S. (2016). Towards catchment classification in data-scarce regions. *Ecohydrology*, *9*, 1235–1247. https://doi.org/10.1002/eco.1721

Aylward, B., Bandyopadhyay, J., Belausteguigotia, J. C., Borkey, P., Cassar, A., Meadors, L., … Tortajada, C. (2005). Freshwater ecosystem services. *Ecosystems and Human Well-Being: Policy Responses*, *3*, 213–256.

Barthem, R. B., Goulding, M., Leite, R. G., Cañas, C., Forsberg, B., Venticinque, E., … Mercado, A. (2017). Goliath catfish spawning in the far western Amazon confirmed by the distribution of mature adults, drifting larvae and migrating juveniles. *Scientific Reports*, *7*, 41784. https://doi.org/10.1038/srep41784

Beauchamp, J. J., Downing, D. J., & Railsback, S. F. (1989). Comparison of regression and time-series methods for synthesizing missing streamflow records. *Journal of the American Water Resources Association*, *25*, 961–975. https://doi.org/10.1111/j.1752-1688.1989.tb05410.x

Bonnet, M. P., Barroux, G., Martinez, J. M., Seyler, F., Moreira-Turcq, P., Cochonneau, G., … Seyler, P. (2008). Floodplain hydrology in an Amazon floodplain lake (Lago Grande de Curuaí). *Journal of Hydrology*, *349*, 18–30. https://doi.org/10.1016/j.jhydrol.2007.10.055

Brinson, M. M. (1993). A hydrogeomorphic classification for wetlands. *Wetlands Research Program Technical Report WRP-DE-4*. Washington, DC: U.S. Army Corps of Engineers, Waterways Experiment Station.

Bunn, S. E., & Arthington, A. H. (2002). Basic principles and ecological consequences of altered flow regimes for aquatic biodiversity.

Environmental Management, *30*, 492–507. https://doi.org/10.1007/s00267-002-2737-0

Cañas, C. M., & Pine, W. E. (2011). Documentation of the temporal and spatial patterns of pimelodidae catfish spawning and larvae dispersion in the Madre de Dios River (Peru): Insights for conservation in the Andean-Amazon headwaters. *River Research and Applications*, *27*, 602–611. https://doi.org/10.1002/rra.1377

Castello, L. (2008). Lateral migration of *Arapaima gigas* in floodplains of the Amazon. *Ecology of Freshwater Fish*, *17*, 38–46. https://doi.org/10.1111/j.1600-0633.2007.00255.x

Castello, L., Isaac, V. J., & Thapa, R. (2015). Flood pulse effects on multi-species fishery yields in the lower Amazon. *Royal Society Open Science*, *2*, 150299. https://doi.org/10.1098/rsos.150299

Castello, L., & Macedo, M. N. (2016). Large-scale degradation of Amazonian freshwater ecosystems. *Global Change Biology*, *22*, 990–1007. https://doi.org/10.1111/gcb.13173

Coe, M. T., Latrubesse, E. M., Ferreira, M. E., & Amsler, M. L. (2011). The effects of deforestation and climate variability on the streamflow of the Araguaia River, Brazil. *Biogeochemistry*, *105*, 119–131. https://doi.org/10.1007/s10533-011-9582-2

Constantine, J. A., Dunne, T., Ahmed, J., Legleiter, C., & Lazarus, E. D. (2014). Sediment supply as a driver of river meandering and floodplain evolution in the Amazon Basin. *Nature Geoscience*, *7*, 899–903. https://doi.org/10.1038/ngeo2282

Coomes, O. T., Lapointe, M., Templeton, M., & List, G. (2016). Amazon River flow regime and flood recessional agriculture: Flood stage reversals and risk of annual crop loss. *Journal of Hydrology*, *539*, 214–222. https://doi.org/10.1016/j.jhydrol.2016.05.027

Coomes, O. T., Takasaki, Y., Abizaid, C., & Barham, B. L. (2010). Floodplain fisheries as natural insurance for the rural poor in tropical forest environments: Evidence from Amazonia. *Fisheries Management and Ecology*, *17*, 513–521. https://doi.org/10.1111/j.1365-2400.2010.00750.x

Correa, S. B., & Winemiller, K. (2018). Terrestrial–aquatic trophic linkages support fish production in a tropical oligotrophic river. *Oecologia*, *186*, 1069–1078. https://doi.org/10.1007/s00442-018-4093-7

Crampton, W. G. R. (2008). Ecology and life history of an Amazon floodplain cichlid: The discus fish *Symphysodon* (Perciformes: Cichlidae). *Neotropical Ichthyology*, *6*, 599–612. https://doi.org/10.1590/s1679-62252008000400008

D'Almeida, C., Vörösmarty, C. J., Hurtt, G. C., Marengo, J. A., Dingman, S. L., & Keim, B. D. (2007). The effects of deforestation on the hydrological cycle in Amazonia: A review on scale and resolution. *International Journal of Climatology*, *27*, 633–647. https://doi.org/10.1002/joc.1475

Davidson, E. A., De Araüjo, A. C., Artaxo, P., Balch, J. K., Brown, I. F., Mercedes, M. M., … Wofsy, S. C. (2012). The Amazon basin in transition. *Nature*, *481*, 321–328. https://doi.org/10.1038/nature10717

de Assis, R. L., & Wittmann, F. (2011). Forest structure and tree species composition of the understory of two central Amazonian várzea forests of contrasting flood heights. *Flora: Morphology, Distribution, Functional Ecology of Plants*, *206*, 251–260. https://doi.org/10.1016/j.flora.2010.11.002

de Paiva, R. C. D., Buarque, D. C., Collischonn, W., Bonnet, M.-P., Frappart, F., Calmant, S., & Bulhões Mendes, C. A. (2013). Large-scale hydrologic and hydrodynamic modeling of the Amazon River basin. *Water Resources Research*, *49*, 1226–1243. https://doi.org/10.1002/wrcr.20067

Dias, M. S., Cornu, J. F., Oberdorff, T., Lasso, C. A., & Tedesco, P. A. (2013). Natural fragmentation in river networks as a driver of speciation for freshwater fishes. *Ecography*, *36*, 683–689. https://doi.org/10.1111/j.1600-0587.2012.07724.x

Do, H. X., Gudmundsson, L., Leonard, M., & Westra, S. (2018). The Global Streamflow Indices and Metadata Archive (GSIM)-Part 1: The production of a daily streamflow archive and metadata. *Earth System Science Data*, *10*, 765–785. https://doi.org/10.5194/essd-10-765-2018

Döll, P., Kaspar, F., & Lehner, B. (2003). A global hydrological model for deriving water availability indicators: Model tuning and validation. *Journal of Hydrology*, *270*, 105–134. https://doi.org/10.1016/s0022-1694(02)00283-4

Domínguez, C. (2004). Importance of rivers for the transportation system of the Amazon. Issues of local and global use of water from the Amazon. UNESCO, Montevideo.

Dunne, T., Mertes, L. A. K., Meade, R. H., Richey, J. E., & Forsberg, B. R. (1998). Exchanges of sediment between the floodplain and channel of the Amazon River in Brazil. *Bulletin of the Geological Society of America*, *110*, 450–467. https://doi.org/10.1130/0016-7606(1998)110<0450:EOSBTF>2.3.CO;2

Encalada, A. C., Flecker, A. S., Poff, N. L. R., Suárez, E., Herrera, G. A., Ríos-Touma, B., … Anderson, E. P. (2019). A global perspective on tropical montane rivers. *Science*, *365*, 1124–1129. https://doi.org/10.1126/science.aax1682

Espinoza Villar, J. C., Ronchail, J., Guyot, J. L., Cochonneau, G., Naziano, F., Lavado, W., … Vauchel, P. (2009). Spatio-temporal rainfall variability in the Amazon basin countries (Brazil, Peru, Bolivia, Colombia, and Ecuador). *International Journal of Climatology*, *29*, 1574–1594. https://doi.org/10.1002/joc.1791

Espinoza Villar, R., Martinez, J. M., Le Texier, M., Guyot, J. L., Fraizy, P., Meneses, P. R., & de Oliveira, E. (2013). A study of sediment transport in the Madeira River, Brazil, using MODIS remote-sensing images. *Journal of South American Earth Sciences*, *44*, 45–54. https://doi.org/10.1016/j.jsames.2012.11.006

Farias, I. P., Willis, S., Leão, A., Verba, J. T., Crossa, M., Foresti, F., … Hrbek, T. (2019). The largest fish in the world's biggest river: Genetic connectivity and conservation of *Arapaima gigas* in the Amazon and Araguaia-Tocantins drainages. *PLoS ONE*, *14*, e0220882. https://doi.org/10.1371/journal.pone.0220882

Fassoni-Andrade, A. C., & de Paiva, R. C. D. (2019). Mapping spatial-temporal sediment dynamics of river-floodplains in the Amazon. *Remote Sensing of Environment*, *221*, 94–107. https://doi.org/10.1016/j.rse.2018.10.038

Filizola, N., & Guyot, J. L. (2009). Suspended sediment yields in the Amazon basin: An assessment using the Brazilian national data set. *Hydrological Processes*, *23*, 3207–3215. https://doi.org/10.1002/hyp.7394

Finer, M., & Jenkins, C. N. (2012). Proliferation of hydroelectric dams in the Andean amazon and implications for Andes-Amazon connectivity. *PLoS ONE*, *7*, e35126. https://doi.org/10.1371/journal.pone.0035126

Fleischmann, A. S., de Paiva, R. C. D., Collischonn, W., Sorribas, M. V., & Pontes, P. R. M. (2016). On river-floodplain interaction and hydrograph skewness. *Water Resources Research*, *52*, 7615–7630. https://doi.org/10.1002/2016wr019233

Freeman, M. C., Pringle, C. M., & Jackson, C. R. (2007). Hydrologic connectivity and the contribution of stream headwaters to ecological integrity at regional scales. *Journal of the American Water Resources Association*, *43*, 5–14. https://doi.org/10.1111/j.1752-1688.2007.00002.x

Getirana, A. C. V., & Paiva, R. C. D. (2013). Mapping large-scale river flow hydraulics in the Amazon Basin. *Water Resources Research*, *49*, 2437–2445. https://doi.org/10.1002/wrcr.20212

Giangrande, S. E., Wang, D., & Mechem, D. B. (2020). Cloud regimes over the Amazon Basin: Perspectives from the GoAmazon2014/5 campaign. *Atmospheric Chemistry and Physics*, *20*, 7489–7507. https://doi.org/10.5194/acp-20-7489-2020

Godoy, R. J., Petts, G., & Salo, J. (1999). Riparian flooded forests of the Orinoco and Amazon basins: A comparative review. *Biodiversity and Conservation*, *8*, 551–586. https://doi.org/10.1023/A:1008846531941

Guimberteau, M., Ronchail, J., Espinoza, J. C., Lengaigne, M., Sultan, B., Polcher, J., … Cais, P. (2013). Future changes in precipitation and impacts on extreme streamflow over Amazonian sub-basins. *Environmental Research Letters*, *8*, e014035. https://doi.org/10.1088/1748-9326/8/1/014035

Gupta, A. (2008). *Large rivers: Geomorphology and management*. Hoboken, NJ: Wiley.

Haaf, E., & Barthel, R. (2018). An inter-comparison of similarity-based methods for organisation and classification of groundwater hydrographs. *Journal of Hydrology*, *559*, 222–237. https://doi.org/10.1016/j.jhydrol.2018.02.035

Hamilton, S. K., Sippel, S. J., & Melack, J. M. (2002). Comparison of inundation patterns among major South American floodplains. *Journal of Geophysical Research: Atmospheres*, *107*, 1–14. https://doi.org/10.1029/2000jd000306

Hannah, D. M., Smith, B. P. G., Gurnell, A. M., & McGregor, G. R. (2000). An approach to hydrograph classification. *Hydrological Processes*, *14*, 317–338. https://doi.org/10.1002/(sici)1099-1085(20000215)14:2<317::aid-hyp929>3.0.co;2-t

Hayes, D. S., Brändle, J. M., Seliger, C., Zeiringer, B., Ferreira, T., & Schmutz, S. (2018). Advancing towards functional environmental flows for temperate floodplain rivers. *Science of the Total Environment*, *633*, 1089–1104. https://doi.org/10.1016/j.scitotenv.2018.03.221

Hennig, C. (2014). fpc: Flexible procedures for clustering. R Package Version 2.1–9.

Hess, L. L., Melack, J. M., Affonso, A. G., Barbosa, C., Gastil-Buhl, M., & Novo, E. M. L. M. (2015). Wetlands of the lowland Amazon basin: Extent, vegetative cover, and dual-season inundated area as mapped with JERS-1 synthetic aperture radar. *Wetlands*, *35*, 745–756. https://doi.org/10.1007/s13157-015-0666-y

Hopkins, W. A. (2007). Amphibians as models for studying environmental change. *ILAR Journal*, *48*, 270–277. https://doi.org/10.1093/ilar.48.3.270

Hwan, J. L., & Holmes, R. W. (2020). Flow regimes in coastal California steelhead trout streams: Spatiotemporal patterns in magnitude, duration and timing. *River Research and Applications*, *36*, 247–258. https://doi.org/10.1002/rra.3571

Iglesias, F., & Kastner, W. (2013). Analysis of similarity measures in times series clustering for the discovery of building energy patterns. *Energies*, *6*, 579–597. https://doi.org/10.3390/en6020579

Isaac, V. J., Castello, L., Santos, P. R. B., & Ruffino, M. L. (2016). Seasonal and interannual dynamics of river-floodplain multispecies fisheries in relation to flood pulses in the lower Amazon. *Fisheries Research*, *183*, 352–359. https://doi.org/10.1016/j.fishres.2016.06.017

Jiménez-Segura, L. F., Palacio, J., & Leite, R. (2010). River flooding and reproduction of migratory fish species in the Magdalena River basin, Colombia. *Ecology of Freshwater Fish*, *19*, 178–186. https://doi.org/10.1111/j.1600-0633.2009.00402.x

Junk, W. J. (2013). Current state of knowledge regarding South America wetlands and their future under global climate change. *Aquatic Sciences*, *75*, 113–131. https://doi.org/10.1007/s00027-012-0253-8

Junk, W. J., Bayley, P., & Sparks, R. (1989). The flood pulse concept in river-floodplain systems. International Large River Symposium, Ontario, Canada.

Junk, W. J., Piedade, M. T. F., Schöngart, J., Cohn-Haft, M., Adeney, J. M., & Wittmann, F. (2011). A classification of major naturally-occurring Amazonian lowland wetlands. *Wetlands*, *31*, 623–640. https://doi.org/10.1007/s13157-011-0190-7

Kahle, D., & Wickham, H. (2019). ggmap: Spatial visualization with ggplot2. *The R Journal*, *5*, 144–161.Retrieved from http://journal.r-project.org/archive/2013-1/kahle-wickham.pdf

Kassambara, A., & Mundt, F. (2019). factoextra: Extract and visualize the results of multivariate data analysis. v1.0.6. Retrieved from http://www.sthda.com/english/rpkgs/factoextra

Knoben, W. J. M., Woods, R. A., & Freer, J. E. (2018). A quantitative hydrological climate classification evaluated with independent streamflow data. *Water Resources Research*, *54*, 5088–5109. https://doi.org/10.1029/2018wr022913

Landeiro, V. L., Bini, L. M., Melo, A. S., Pes, A. M. O., & Magnusson, W. E. (2012). The roles of dispersal limitation and environmental conditions in controlling caddisfly (Trichoptera) assemblages. *Freshwater Biology*, *57*, 1554–1564. https://doi.org/10.1111/j.1365-2427.2012.02816.x

Lane, B. A., Sandoval-Solis, S., Stein, E. D., Yarnell, S. M., Pasternack, G. B., & Dahlke, H. E. (2018). Beyond metrics? The role of hydrologic baseline archetypes in environmental water management. *Environmental Management*, *62*, 678–693. https://doi.org/10.1007/s00267-018-1077-7

Laraque, A., Ronchail, J., Cochonneau, G., Pombosa, R., & Guyot, J. L. (2007). Heterogeneous distribution of rainfall and discharge regimes in the Ecuadorian Amazon basin. *Journal of Hydrometeorology*, *8*, 1364–1381. https://doi.org/10.1175/2007jhm784.1

Larson, E. (2019). *The structural and functional consequences of disturbance on biodiversity in tropical and temperate montane streams* (PhD Thesis). Cornell University, Ithaca, NY, USA.

Leigh, C., Stewart-Koster, B., Sheldon, F., & Burford, M. A. (2012). Understanding multiple ecological responses to anthropogenic disturbance: Rivers and potential flow regime change. *Ecological Applications*, *22*, 250–263. https://doi.org/10.1890/11-0963.1

Lessmann, J., Troya, M. J., Flecker, A. S., Funk, W. C., Guayasamin, J. M., Ochoa-Herrera, V., … Encalada, A. C. (2019). Validating anthropogenic threat maps as a tool for assessing river ecological integrity in Andean-Amazon basins. *PeerJ*, *7*, e8060. https://doi.org/10.7717/peerj.8060

Levy, M. C., Lopes, A. V., Cohn, A., Larsen, L. G., & Thompson, S. E. (2018). Land use change increases streamflow across the arc of deforestation in Brazil. *Geophysical Research Letters*, *45*, 3520–3530. https://doi.org/10.1002/2017gl076526

Liebmann, B., & Marengo, J. A. (2001). Interannual variability of the rainy season and rainfall in the Brazilian Amazon Basin. *Journal of Climate*, *14*, 4308–4318. https://doi.org/10.1175/1520-0442(2001)014<4308:ivotrs>2.0.co;2

Lilly, A. (2010). A hydrological classification of UK soils based on soil morphological data. Proceedings of the 19th World Congress of Soil Science: Soil solutions for a changing world, Brisbane, Australia.

Lima, L. S., Coe, M. T., Soares Filho, B. S., Cuadra, S. V., Dias, L. C. P., Costa, M. H., … Rodrigues, H. O. (2014). Feedbacks between deforestation, climate, and hydrology in the Southwestern Amazon: Implications for the provision of ecosystem services. *Landscape Ecology*, *29*, 261–274. https://doi.org/10.1007/s10980-013-9962-1

Lowe-McConnell, R. (2011). Historical biogeography of neotropical freshwater fishes. *Historical Biogeography of Neotropical Freshwater Fishes*, *105*, 253–254. https://doi.org/10.1111/j.1095-8312.2011.01766.x

Malhado, A. C. M., Pires, G. F., & Costa, M. H. (2010). Cerrado conservation is essential to protect the Amazon rainforest. *Ambio*, *39*, 580–584. https://doi.org/10.1007/s13280-010-0084-6

Marengo, J. A. (2004). Interdecadal variability and trends of rainfall across the Amazon basin. *Theoretical and Applied Climatology*, *78*, 79–96. https://doi.org/10.1007/s00704-004-0045-8

Marengo, J. A., & Espinoza, J. C. (2016). Extreme seasonal droughts and floods in Amazonia: Causes, trends and impacts. *International Journal of Climatology*, *36*, 1033–1050. https://doi.org/10.1002/joc.4420

Mayorga, E., Logsdon, M. G., Ballester, M. V. R., & Richey, J. E. (2012). *LBA-ECO CD-06 Amazon River basin land and stream drainage direction maps* [Data set]. Retrieved from http://daac.ornl.gov

McClain, M. E., & Naiman, R. J. (2008). Andean influences on the biogeochemistry and ecology of the Amazon River. *Bioscience*, *58*, 325–338. https://doi.org/10.1641/b580408

McMillan, H., Westerberg, I., & Branger, F. (2017). Five guidelines for selecting hydrological signatures. *Hydrological Processes*, *31*, 4757–4761. https://doi.org/10.1002/hyp.11300

Melack, J. M., & Hess, L. L. (2010). Remote sensing of the distribution and extent of wetlands in the Amazon basin. In W. Junk, M. Piedade, F. Wittmann, J. Schöngart, & P. Parolin (Eds.), *Amazonian floodplain forests. Ecological studies (analysis and synthesis)* (Vol. 210, pp. 43–59). Dordrecht: Springer.

Mertes, L. A. K., Daniel, D. L., Melack, J. M., Nelson, B., Martinelli, L. A., & Forsberg, B. R. (1995). Spatial patterns of hydrology, geomorphology, and vegetation on the floodplain of the Amazon River in Brazil from a remote sensing perspective. *Geomorphology*, *13*, 215–232. https://doi.org/10.1016/0169-555x(95)00038-7

Miranda-Chumacero, G., Álvarez, G., Luna, V., Wallace, R. B., & Painter, L. (2015). First observations on annual massive upstream migration of juvenile catfish *Trichomycterus* in an Amazonian River. *Environmental Biology of Fishes*, *98*, 1913–1926. https://doi.org/10.1007/s10641-015-0407-3

Nature Conservancy. (2009). Indicators of hydrologic alteration software version 7.1 user's manual.

NEON. (2020). Retrieved from http://neonscience.org

Nepstad, D. C., Tohver, I. M., David, R., Moutinho, P., & Cardinot, G. (2007). Mortality of large trees and lianas following experimental drought in an Amazon forest. *Ecology*, *88*, 2259–2269. https://doi.org/10.1890/06-1046.1

Oberdorff, T., Dias, M. S., Jézéquel, C., Albert, J. S., Arantes, C. C., Bigorne, R., … Zuanon, J. (2019). Unexpected fish diversity gradients in the Amazon basin. *Science Advances*, *5*, eeav8681. https://doi.org/10.1126/sciadv.aav8681

Olden, J. D., Kennard, M. J., & Pusey, B. J. (2012). A framework for hydrologic classification with a review of methodologies and applications in ecohydrology. *Ecohydrology*, *5*, 503–518. https://doi.org/10.1002/eco.251

Olden, J. D., & Poff, N. L. (2003). Redundancy and the choice of hydrologic indices for characterizing streamflow regimes. *River Research and Applications*, *19*, 101–121. https://doi.org/10.1002/rra.700

Ouellet-Dallaire, C., Lehner, B., Sayre, R., & Thieme, M. (2019). A multi-disciplinary framework to derive global river reach classifications at high spatial resolution. *Environmental Research Letters*, *14*, 024003. https://doi.org/10.1088/1748-9326/aad8e9

Palmer, M., & Ruhi, A. (2019). Linkages between flow regime, biota, and ecosystem processes: Implications for river restoration. *Science*, *365*, eeaw2087. https://doi.org/10.1126/science.aaw2087

Parolin, P. (2012). Diversity of adaptations to flooding in trees of Amazonian floodplains. *Pesquisas Botanica*, *63*, 7–28.

Pfafstetter, O. (1989). Classification of hydrographic basins: Coding methodology. Unpublished manuscript, Departmento Nacional de Obras de Saneamento, Rio de Janeiro.

Poff, N. L., Allan, J. D., Bain, M. B., Karr, J. R., Prestegaard, K. L., Richter, B. D., … Stromberg, J. C. (1997). The natural flow regime. *Bioscience*, *47*, 769–784. https://doi.org/10.2307/1313099

Poff, N. L., Richter, B. D., Arthington, A. H., Bunn, S. E., Naiman, R. J., Kendy, E., … Warner, A. (2010). The ecological limits of hydrologic alteration (ELOHA): A new framework for developing regional environmental flow standards. *Freshwater Biology*, *55*, 147–170. https://doi.org/10.1111/j.1365-2427.2009.02204.x

Poff, N. L., & Zimmerman, J. K. H. (2010). Ecological responses to altered flow regimes: A literature review to inform the science and management of environmental flows. *Freshwater Biology*, *55*, 194–205. https://doi.org/10.1111/j.1365-2427.2009.02272.x

Polato, N. R., Gill, B. A., Shah, A. A., Gray, M. M., Casner, K. L., Barthelet, A., … Zamudio, K. R. (2018). Narrow thermal tolerance and low dispersal drive higher speciation in tropical mountains. *Proceedings of the National Academy of Sciences of the United States of America*, *115*, 12471–12476. https://doi.org/10.1073/pnas.1809326115

RAISG: Red Amazónica de Información Socioambiental Georreferenciada. (2012). Retrieved from https://www.amazoniasocioambiental.org/

Renöfält, B. M., Jansson, R., & Nilsson, C. (2010). Effects of hydropower generation and opportunities for environmental flow management in Swedish riverine ecosystems. *Freshwater Biology*, *55*, 49–67. https://doi.org/10.1111/j.1365-2427.2009.02241.x

Richter, B. D., Baumgartner, J. V., Powell, J., & Braun, D. P. (1996). A method for assessing hydrologic alteration within ecosystems. *Conservation Biology*, *10*, 1163–1174. https://doi.org/10.1046/j.1523-1739.1996.10041163.x

Ríos-Villamizar, E. A., Piedade, M. T. F., Da Costa, J. G., Adeney, J. M., & Junk, W. J. (2013). Chemistry of different Amazonian water types for river classification: A preliminary review. *WIT Transactions on Ecology and the Environment*, *178*, 17–28. https://doi.org/10.2495/ws130021

Salati, E., & Vose, P. B. (1984). Amazon basin: A system in equilibrium. *Science*, *225*, 129–138. https://doi.org/10.1126/science.225.4658.129

Sioli, H. (1957). Sedimentation in the Amazon. *Geological Survey*, *45*, 608–633. https://doi.org/10.1007/bf02296856

Snelder, T. H., Biggs, B. J. F., & Woods, R. A. (2005). Improved eco-hydrological classification of rivers. *River Research and Applications*, *21*, 609–628. https://doi.org/10.1002/rra.826

Solans, M., & Poff, N. (2013). Classification of natural flow regimes in the Ebro basin (Spain) by using a wide range of hydrologic parameters. *River Research and Applications*, *29*, 1147–1163. https://doi.org/10.1002/rra.2598

Sousa, R. G. C., & Freitas, C. E. D. C. (2008). The influence of flood pulse on fish communities of floodplain canals in the middle Solimões River, Brazil. *Neotropical Ichthyology*, *6*, 249–255. https://doi.org/10.1590/s1679-62252008000200013

Tibshirani, R., Walther, G., & Hastie, T. (2001). Estimating the number of clusters in a data set via the gap statistic. *Journal of the Royal Statistical Society. Series B: Statistical Methodology*, *63*, 411–423. https://doi.org/10.1111/1467-9868.00293

Timpe, K., & Kaplan, D. (2017). The changing hydrology of a dammed Amazon. *Science Advances*, *3*, e1700611. https://doi.org/10.1126/sciadv.1700611

Valle, D., & Kaplan, D. (2019). Quantifying the impacts of dams on riverine hydrology under non-stationary conditions using incomplete data and Gaussian copula models. *Science of the Total Environment*, *677*, 599–611. https://doi.org/10.1016/j.scitotenv.2019.04.377

Vannote, R. L., Minshall, G. W., Cummins, K. W., Sedell, J. R., & Cushing, C. E. (1980). The river continuum concept. *Canadian Journal of Fisheries and Aquatic Sciences*, *37*, 130–137. https://doi.org/10.1139/f80-017

Venticinque, E., Forsberg, B., Barthem, R., Petry, P., Hess, L., Mercado, A., … Goulding, M. (2016). An explicit GIS-based river basin framework for aquatic ecosystem conservation in the Amazon. *Earth System Science Data*, *8*, 651–661. https://doi.org/10.5194/essd-8-651-2016

Ward, J. H. (1963). Hierarchical grouping to optimize an objective function. *Journal of the American Statistical Association*, *58*, 236–244. https://doi.org/10.1080/01621459.1963.10500845

Werth, D. (2002). The local and global effects of Amazon deforestation. *Journal of Geophysical Research*, *107*, 1–8. https://doi.org/10.1029/2001jd000717

Winemiller, K. O., McIntyre, P. B., Castello, L., Fluet-Chouinard, E., Giarrizzo, T., Nam, S., … Sáenz, L. (2016). Balancing hydropower and biodiversity in the Amazon, Congo, and Mekong. *Science*, *351*, 128–129. https://doi.org/10.1126/science.aac7082

Wohl, E., Barros, A., Brunsell, N., Chappell, N. A., Coe, M., Giambelluca, T., … Ogden, F. (2012). The hydrology of the humid tropics. *Nature Climate Change*, *2*, 655–662. https://doi.org/10.1038/nclimate1556

Yarnell, S. M., Stein, E. D., Webb, J. A., Grantham, T., Lusardi, R. A., Zimmerman, J., … Sandoval-Solis, S. (2020). A functional flows approach to selecting ecologically relevant flow metrics for environmental flow applications. *River Research and Applications*, *36*, 318–324. https://doi.org/10.1002/rra.3575

SUPPORTING INFORMATION

Additional supporting information may be found online in the Supporting Information section at the end of this article.

How to cite this article: Siddiqui SF, Zapata-Rios X, Torres-Paguay S, et al. Classifying flow regimes of the Amazon basin. *Aquatic Conserv: Mar Freshw Ecosyst*. 2021;1–24. https://doi.org/10.1002/aqc.3582